FURTHER CHARACTERIZATION OF CLOSED PORE INSULATION (CPI)

by

Michael Russak and Carl Feldman

Research Department
Grumman Aerospace Corporation
Bethpage, New York 11714

RE-455

Final Report on Extension to
Contract NAS 1-10713

Prepared for
Langley Research Center
Langley Station
Hampton, Virginia 23365

May 1973

NATIONAL AERONAUTICS AND SPACE ADMINISTRATION

FURTHER CHARACTERIZATION OF CLOSED PORE INSULATION (CPI)

by

Michael Russak and Carl Feldman

Research Department
Grumman Aerospace Corporation
Bethpage, New York 11714

Final Report on Extension to
Contract NAS 1-10713

Prepared for
National Aeronautics and Space Administration
Langley Research Center
Langley Station
Hampton, Virginia 23365

May 1973

Approved by: Charles E. Mack, Jr.
Charles E. Mack, Jr.
Director of Research

ACKNOWLEDGMENTS

The authors wish to thank Dr. Albert Tobin and Mr. Joseph Reichman of the Grumman Research Department for their helpful suggestions and contributions during this study. We are also indebted to Messrs. Guenter Baumann, John Jenkins, George McLaughlin, Herman Behan, and Robert Anderson of the Grumman Materials and Processes Department, for their preparation and heat treatment of the CPI tiles and samples. Many thanks also go to Mr. Richard Truran of the Grumman Materials Test Laboratory for his measurement of the mechanical properties of CPI, and to Messrs. John Androulakis and Charles Dunkerly of the Grumman Thermal and Environmental Test Laboratory for their measurement of the thermal properties and performance of the re-entry thermal cycling on the CPI materials.

SUMMARY

The thermophysical and mechanical properties of Closed Pore Insulation (CPI) were measured after exposure to 25 simulated re-entry thermal cycles. In addition, mechanical properties were obtained at elevated temperatures before and after cycling. The properties of CPI were not compromised by the cycling.

High temperature creep studies were done on three CPI compositions (4, 8, and 12 Wt% CoO additive). CPI-4 had the best creep resistance at temperatures up to 1363 K.

TABLE OF CONTENTS

LIST OF ILLUSTRATIONS

LIST OF TABLES

I. INTRODUCTION

The primary objective of this work is further characterization of Grumman's closed pore insulation (CPI) as a candidate heat shield material for the Space Shuttle Orbiter. Room temperature properties of CPI were initially characterized under NASA Contract NAS 1-10713 (Ref. 1). The program carried out herein included measurement of thermophysical and mechanical properties of CPI at elevated temperatures before and after 25 simulated re-entry thermal cycles. The purpose of these experiments was to determine the extent of degradation, if any, of CPI after exposure to the re-entry thermal environment.

II. SIMULATED RE-ENTRY THERMAL CYCLING

A programmed quartz lamp array was used to simulate the re-entry temperature profile. The details of this experimental setup have been given previously (Ref. 1). The time-temperature re-entry profiles used in this study are shown in Fig. 1. These profiles were based on the most recent re-entry trajectory heat fluxes from NASA-MSC and are more realistic than the trapezoidal cycle used in earlier work (Ref. 1), which are also shown in Fig. 1. The test pieces were nominally 20 cm x 20 cm x 1 cm. Two CPI-12 tiles were cycled 25 times through Area 1 and two CPI-8 tiles were cycled 25 times through Area 2. CPI-4 characterized under NASA Contract NAS 9-12781 can be used for Areas 1, 2, and 2P. Some of the results obtained on this material are included in this report. The cycled tiles were then machined as shown in Fig. 2 into the sample configurations necessary for the testing program.

III. THERMOPHYSICAL PROPERTIES

A. Density and Physical Dimensions

Tables 1 and 2 compare the densities and physical dimensions of the CPI tiles before and after re-entry cycling. The data indicate that both compositions remained dimensionally stable during cycling. Minor differences in dimensions and densities were found not to be statistically significant.

B. Microstructure

The foamlike structure of CPI-12 and CPI-8 was not altered by the simulated re-entry thermal cycling. Figure 3 shows micrographs of CPI-12 and CPI-8 after re-entry cycling. No statistical difference in the pore sizes was observed before and after cycling. CPI-12 had an average pore size of 300μm and CPI-8 had an average pore size of 175μm.

The X-ray diffractograms of the cycled and uncycled tiles showed that there was no change in the relative amounts of cobalt aluminate, mullite, and glass, indicating the materials remained chemically stable during cycling. There were no noticeable color changes in the materials.

C. Water Absorption

Measurements of water absorption were made by immersing the samples (nominally 2 cm x 2 cm x 2 cm) for 96 hours in a beaker of water at room temperature before and after thermal cycling. It was necessary to put weights on the samples to keep them submerged. Following removal from the beaker, they were dipped in alcohol to remove any surface water, and then reweighed. The water absorption was then calculated according to the following formula:

$$\% \text{ WA} = \text{Wt. gained/Dry Wt. of Block X100}$$

Table 3 summarizes the water absorption data. It can be seen from these data that re-entry thermal cycling did not compromise the waterproof characteristics of CPI. The variation in percent water absorption is not statistically significant.

Table 1

PHYSICAL DIMENSIONS AND DENSITIES OF CPI-12 AND CPI-8 TILES BEFORE THERMAL CYCLING

Tile	L (cm)	W (cm)	H (cm)	Density (Kg/m^3)	Density (pcf)
A-1	19.8	20.3	0.96	635.09	39.63
A-2	18.4	17.6	1.02	647.35	40.40
B-1	20.1	20.4	1.00	612.33	38.21
B-2	19.4	21.0	0.98	671.95	41.93

Table 2

PHYSICAL DIMENSIONS AND DENSITIES OF CPI-12 AND CPI-8 TILES AFTER THERMAL CYCLING

Tile	L (cm)	W (cm)	H (cm)	Density (Kg/m^3)	Density (pcf)
A-1	19.8	20.2	0.96	636.85	39.74
A-2	18.4	17.6	1.01	647.11	40.38
B-1	20.0	20.3	1.00	610.57	38.10
B-2	19.4	20.9	0.99	670.51	41.84

A = CPI-12

B = CPI-8

D. Thermal Expansion

Linear thermal expansion measurements were made on the CPI-12 and CPI-8 material before and after cycling. A fused quartz dilatometer was used and the slope of the percent linear expansion versus temperature curve in the temperature region of 298 to 1073 K was taken as the average linear coefficient of thermal expansion. The dilatometric softening points (Mg point) were also extracted from these curves. The coefficients of thermal expansion and the Mg points are tabulated in Table 4. It can be seen that the simulated re-entry thermal cycling did not affect the thermal expansions nor the Mg points.

E. Thermal Conductivity

Thermal conductivity was measured using a radial heat flow method previously described (Ref. 1). Figures 4 and 5 show the data obtained from these measurements. There was no apparent change in the thermal conductivities after cycling (within the six percent error of the measuring apparatus).

F. Total Normal Emittance

The total normal emittance apparatus has also been previously detailed (Ref. 1). Figures 6 and 7 show the total normal emittance of CPI-12 and CPI-8 before and after cycling. There was a slight increase in emittance of both these materials after cycling. This may be due to an improvement in the measuring technique in the time interval between the runs. It should also be noted that there is approximately a seven percent error bar on these measurements. The emittance of both CPI-12 and CPI-8 was not lowered by the simulated re-entry thermal cycling.

Table 3

WATER ABSORPTION OF CPI-12 AND CPI-8 BEFORE AND AFTER THERMAL CYCLING

Tile	% Water Absorption Uncycled	% Water Absorption Cycled
A-1	1.03	1.10
A-2	0.09	0.07
B-1	1.43	1.38
B-2	1.01	0.97

A = CPI-12

B = CPI-8

Table 4

THERMAL EXPANSION COEFFICIENTS AND Mg POINTS FOR CPI-12 AND CPI-8 BEFORE AND AFTER CYCLING

Composition	Coefficient of Linear Thermal† Expansion (10^{-6}/K)		Mg Point (K)†	
	Uncycled	Cycled	Uncycled	Cycled
CPI-12	5.80	5.82	1184	1179
CPI-8	5.46	5.42	1254	1260

†Average values of three runs

IV. MECHANICAL PROPERTIES

Another objective of this work was to determine the effect of cycling on the mechanical properties of CPI, as well as the evaluation of mechanical properties of CPI-12 and CPI-8 at elevated temperatures. The program consisted of the determination of the flexural, tensile, and compressive properties of the subject material at room and elevated temperatures, both before and after thermal cycling. Flexural tests employed a simple beam under center point loading. Tensile determinations were made by using a diametral compression load applied to a disk-shaped specimen. Edgewise loading of a free standing prismatic specimen was used to determine the compression properties. A detailed description of the room temperature testing apparatus and procedures has been given (Ref. 1).

The elevated temperature mechanical testing was conducted using a platinum-wound, 12-cm-diameter, resistance heated furnace suspended under the movable crosshead of a universal testing machine (Fig. 8). With this arrangement it was possible to lower the preheated furnace gradually to the specimen, which was supported on an alumina fixture. The rate of furnace descent, controlled by the crosshead velocity of the machine, determined the heating rate of the specimen and fixtures. The rate of temperature rise was held to 100 K per minute. Once the specimen was in the constant temperature zone of the furnace, it was allowed to stabilize for 15 minutes before testing. The samples were loaded by using a solid alumina rod threaded into the load cell of the testing machine. Figures 8 to 14 show the experimental apparatus and fixturing in detail. The original elevated temperature testing program called for characterization of CPI-12 and CPI-8 in the temperature range of 1273 to 1473 K. However, initial results indicated that mechanical property data in this temperature range were not meaningful due to viscous flow of the CPI. As reported earlier, (Table 4) the Mg points of CPI-12 and CPI-8 were found to be 1180 and 1260 K, respectively. At temperatures below these softening points, brittle failures were encountered at relatively low strain rates [< 0.4 cm/min (0.15 in/min)]. However, at higher temperatures, the failure of CPI-12 and CPI-8 becomes strain-rate dependent and higher strain rates [> 5 cm/min (2 in./min)] were necessary to produce brittle failures. At lower loading rates, the material behaves plastically. At 1273 K, CPI-8 supported a stress of 4.12×10^6 N/m^2 (600 psi) using a strain rate of 2.54 cm/min, and at 1373 K it supported 1.38×10^6 N/m^2 (200 psi) at the same strain rate. It was realized that these high

strain rates were not indicative of launch or re-entry loading and the mechanical testing program was modified. Mechanical testing, therefore, was done below 1223 K to eliminate the strain rate dependence. This testing program is outlined in Table 5. A strain rate of 0.3 cm/min (0.12 in./min) was used in all testing. This strain rate provided a basis of comparison for the data and assured brittle failures at the chosen test temperature. At temperatures above the softening range, creep studies were carried out. These experiments are described fully in the next section of this report. The results of this testing program are summarized in Table 6 and are presented graphically in Figs. 15 to 20. The unreduced mechanical property data are presented in the appendix. It can be seen from these data that there was no drastic degradation of the mechanical properties of CPI-12 and CPI-8 due to re-entry thermal cycling. The increase in properties observed at 900 K for several tests is believed to be due to annealing effects in the CPI, whereby any stresses induced in the samples due to machining etc. are relieved when the sample is heated in this temperature range.

Table 5

CPI HIGH TEMPERATURE TESTING PROGRAM

Test Temperature		Number of Specimens in Each Test Shown					
		CPI-12			CPI-8		
K	°F	Flexure	Compression	Tension	Flexure	Compression	Tension
	Uncycled						
298	70	*	*	*	*	*	*
900	1160	3	3	3	3	3	3
1125	1570	3	3	3	3	3	3
	Cycled						
298	70	3	3	3	3	3	3
900	1160	3	3	3	3	3	3
1125	1570	3	3	3	3	3	3

*Data generated earlier (Ref. 1)

Table 6

SUMMARY OF AVERAGE MECHANICAL PROPERTIES OF CPI-8 AND CPI-12

Property	CPI-8						CPI-12					
	Strength (N/m^2)			Modulus (N/m^2)			Strength (N/m^2)			Modulus (N/m^2)		
	R.T.	900K	1125 K	R.T.	900K	1125K	R.T.	900K	1125K	R.T.	900K	1125K
Flexure												
Uncycled	5.9×10^6	6.9×10^6	5.6×10^6	5.6×10^9	6.2×10^9	2.3×10^9	5.7×10^6	8.2×10^6	7.5×10^6	6.4×10^9	7.5×10^9	4.8×10^9
Cycled	6.2	6.9	6.0	6.4	4.8	3.1	7.5	8.2	6.5	8.2	6.5	4.1
Tensile (Diametral Compression)												
Uncycled	4.0	3.5	1.9	-	-	-	4.7	3.8	2.9	-	-	-
Cycled	4.1	4.1	3.9	-	-	-	4.9	3.1	2.3	-	-	-
Edgewise Compression												
Uncycled	24.8	17.9	11.7	-	-	-	28.9	22.7	17.2	-	-	-
Cycled	22.0	21.3	17.2	-	-	-	23.4	10.3	12.4	-	-	-

V. CREEP STUDY

High temperature creep experiments were carried out to evaluate CPI for various mechanically attached standoff heat shield design concepts being considered under Contract NAS 9-12781 (Ref. 2). Because of the glassy behavior of CPI, as well as its strain rate dependence at temperatures above the dilatometric softening point, it was believed that it would be more meaningful to establish the creep characteristics of the material under uniform pressure loading at various temperatures.

The sample configuration for this test was a beam 16.5 cm x 1.3 cm x 0.6 cm (6.50" x 0.50" x 0.25") that was stressed to 6.9×10^2 N/m^2 (0.1 psi) to simulate re-entry loading. A 15.3-cm (6.00") loading span was used. Loading was accomplished by equally spacing cylindrical alumina weights across the loading span. This uniform load translated to an extreme fiber stress of 2.95×10^5 N/m^2 (43 psi). The loaded beam was supported at the ends in a box furnace that was then brought to the desired soak temperature. Three loaded beams were used for each test. Figure 21 shows the experimental setup prior to testing. The combination of temperatures and compositions used in the creep study are presented in Table 7. The beams were held for approximately 20 hours at each test temperature with beam deflection versus time

Table 7

COMBINATIONS USED IN CREEP STUDY

Composition Wt.% CoO	Temperature K			
	1033	1143	1253	1368
4	✓		✓	✓
8	✓	✓	✓	
12	✓	✓	✓	

monitored photographically. Figure 22 shows the CPI-8 samples after 18 hours at 1253 K (1800°F). A radius gauge was used to obtain the radii of curvature of the deflected beams at various times. The radius of curvature and creep strain are related by (Ref. 3):

$$\epsilon_c = \frac{1}{8}\left(\frac{1}{R}\right)$$

where

ϵ_c = creep strain

$\frac{1}{R}$ = radius of curvature

$\frac{1}{8}$ = geometric factor

From this relation, the creep strain versus time was determined for each test temperature. These data are summarized in Table 8. Figure 23 shows the flexural creep strain curve for CPI-8 at 1253 K. From the accumulated creep data, it was determined that in an unsupported standoff heat shield panel design, CPI-4 is usable for Areas 2P, 2, and 1 while CPI-8 is best suited for Areas 2 and 1, and CPI-12 is most reliable in Area 1. It should be noted that this study used beams with a thickness of 0.6 cm, whereas in the more detailed design work done under NASA Contract NAS 9-12781, CPI was used in thicknesses of 1.8 cm. This increased thickness gives an increase in use temperature of approximately 100 K (~ 200°F). It should be further noted that these tests were run isothermally, whereas under actual re-entry conditions a thermal gradient would exist through the material that would also tend to limit creep effects.

Table 8

CREEP STRAIN (10^{-3}) VERSUS TIME FOR CPI-4, CPI-8, and CPI-12

(Time, Hrs)

Temperature	0	0.5	1.0	1.5	2.0	2.5	3.0	3.5	4.0	18.0	20	21
CPI-4												
1368 K	0	0.94	2.36	4.10	5.37	5.37	5.37	5.37	-	12.9	-	-
1253		Zero	Creep	Strain								
1143		Zero	Creep	Strain								
1033		Zero	Creep	Strain								
CPI-8												
1253	0	2.68	6.76	6.76	9.15	-	-	-	-	12.1	-	-
1143	0	0	0	0	0	0	0	0	0.15	-	0.15	-
1033		Zero	Creep	Strain								
CP-12												
1253	0	9.80	15.60	21.50	21.50	23.60	*					
1143	0	-	0.08	0.20	0.34	-	0.35	0.78	0.78	-	-	3.58
1033		Zero	Creep	Strain								

*Samples bottomed out in fixture, test terminated

VI. RESULTS AND CONCLUSIONS

This study resulted in the further characterization of CPI-12 and CPI-8 by measurement of their thermophysical and mechanical properties at elevated temperatures before and after simulated re-entry cycling. Useful heat shield design information was obtained through elevated temperature creep measurements. The data generated in this work have shown that the re-entry thermal environment has no detrimental effects on these materials. It has also been established that CPI-12 and CPI-8 can be used in mechanically attached, standoff heat shield components as well as in bonded schemes with fibrous insulations.

In summary, the following conclusions are stated:

1. Scaled-up (20 cm x 20 cm x 1 cm) CPI-12 and CPI-8 tiles have been successfully cycled through 25 re-entry thermal cycles of Area 1 and 2, respectively.

2. CPI-12 and CPI-8 were physically and chemically stable during and after cycling.

3. CPI-12 and CPI-8 maintained their waterproof characteristics after cycling.

4. The coefficient of thermal expansion, thermal conductivity, and total normal emittance of CPI-12 and CPI-8 were not changed as a result of re-entry thermal cycling.

5. No decrease in room temperature or elevated temperature mechanical properties (flexural, compressive, tensile, and Young's modulus) was found in CPI-12 and CPI-8 after thermal cycling.

6. A strain rate dependence of brittle failures in CPI-12 and CPI-8 was found at temperatures above their respective dilatometric softening points.

7. The high temperature creep study showed that CPI-12 and CPI-8 could be used in unsupported mechanically attached stand-off heat shield designs for use in Areas 1 and 2, respectively.†

†Details will be published in the final report for NASA Contract NAS 9-12781.

REFERENCES

1. Tobin, A., Feldman, C., Russak, M., and Reichman, J., Development of a Closed Pore Insulation Material, Grumman Aerospace Corporation, Final Report on Contract NAS 1-10713, February 1972.

2. Varisco, A. and Harris, H., "CPI Design Integration," Symposium on Reusable Surface Insulation for Space Shuttle, Ames Research Center, Moffett Field, California, November 1-3, 1972.

3. Timoshenko, S., Strength of Materials, Van Nostrand Company, Princeton, New Jersey, 1963.

APPENDIX

MECHANICAL PROPERTY DATA FOR CPI-12 AND CPI-8

Table A-1

FLEXURAL PROPERTIES OF CPI MATERIAL WITH 8 AND 12 PERCENT COBALT ADDITIVE

Spec. Ident.	Test Temp. (°C)	Thick (in.)	Width (in.)	Fail Load (lbs)	Ult. Stress (psi)	Mod x 10^6 (psi)	Location of Failure	
							Center	Off-Center
				GROUP I - 8% Cobalt				
				A - Uncycled				
S5-1	R.T.	.242	.626	4.45	725	.79	✓	
-4		.243	.626	5.42	880	.84		✓
-5		.243	.626	5.94	963	.84	✓	
					Avg. 860	.82		
U -4	620	.250	.520	7.40	1020	.95	✓	
-5		.250	.520	7.40	1020	.90	✓	
-6		.250	.519	7.22	1000	.82	✓	
					Avg. 1000	.90		
U -1	850	.250	.520	5.95	824	.35	✓	
-2		.250	.519	6.08	843	.35	✓	
-3		.250	.519	5.62	780	.35	✓	
					Avg. 820	.34		
				B - Cycled - 25 ~ Area 2				
C -1	R.T.	.263	.496	7.27	893	.96	✓	
-2		.263	.496	7.74	951	.92	✓	
-3		.263	.496	7.16	879	.90	✓	
-4		.263	.496	7.44	914	.93		
					Avg. 900	.93		
C -5	620	.263	.496	8.42	1110	.73	✓	
-6		.261	.496	7.60	1030	.76	✓	
-7		.263	.496	7.45	980	.61	✓	
					Avg. 1000	.70		
C -8	850	.262	.500	7.54	985	.43	✓	
-9		.264	.496	8.00	1040	.47	✓	
-10		.264	.496	4,52(*)	610	.46		✓
					Avg. 880	.45		
				GROUP II - 12% Cobalt				
				A - Uncycled				
U -1	R.T.	.314	.640	8.35	893	1.05	✓	
-2		.270	.645	5.15	739	.78		✓
-3		.269	.643	5.45	790	.92	✓	
-4		.269	.657	6.10	865	.96	✓	
-5		.266	.659	5.80	839	.95	✓	
-6		.271	.655	6.00	842	.91	✓	
					Avg. 830	.93		
U -1	620	.251	.469	7.70	1173	1.10	✓	
-2		.251	.465	7.71	1183	1.15	✓	
-3		.251	.454	7.62	1200	1.12	✓	
					Avg. 1200	1.10		
U -4	850	.251	.456	7.40	1158	.71	✓	
-5		.251	.461	7.35	1136	.70	✓	
		.251	.460	7.49	1161	.64	✓	
					Avg. 1100	.70		
				B - Cycled - 25 ~ Area 1				
C -1	R.T.	.252	.495	6.12	875	1.20	✓	
-2		.252	.497	8.20	1170	1.18	✓	
-3		.252	.497	8.35	1190	1.17	✓	
					Avg. 1100	1.20		
C -4	620	.252	.496	8.70	1240	.98	✓	
-5		.252	.493	7.40	1170	.92	✓	
					Avg. 1200	.95		
C -6	850	.252	.496	6.52	930	.64	✓	
-7		.252	.498	6.80	970	.60	✓	
					Avg. 950	.60		

*Large void noted in test section.

Table A-2

DIAMETRAL COMPRESSION PROPERTIES OF CPI MATERIAL WITH 8 AND 12 PERCENT COBALT ADDITIVE

Spec. Ident.	Test Temp. (°C)	Thick (in.)	Diameter (in.)	Fail Load (lbs)	Ult. Tensile Stress (psi)	Mode of Failure: Triple Cleft	Mode of Failure: Tension
			GROUP I - 8% Cobalt				
			A - Uncycled				
U -7	R.T.	.537	1.279	615	570	✓	
-8		.542		672	617	✓	
					Avg. 590		
U -1	620	.542	1.279	600	553		✓
-2		.541		594	546		✓
-3		.542		475	436	✓	
					Avg. 512		
U -4	850	.544	1.279	294	270	✓	
-5		.537		346	321	✓	
-6		.543		249	228	✓	
					Avg. 270		
			B - Cycled - 22 ~ Area 2				
C -1	R.T.	.376	1.282	510	674	✓	
-2		.380		420	549	✓	
-3		.377		448	590	✓	
					Avg. 600		
C -4	620	.378	1.282	472	620	✓	
-5		.379		430	564	✓	
-6		.380		465	608	✓	
					Avg. 597		
C -7	850	.380	1.282	524	680	✓	
-8		.379		415	540	✓	
-9		.380		372	485	✓	
					Avg. 570		
			GROUP II - 12% Cobalt				
			A - Uncycled				
U -7	R.T.	.475	1.280	676	708	✓	
-8		.462	1.279	616	664	✓	
-9		.458	1.279	654	710	✓	
					Avg. 690		
U -1	620	.441	1.279	443	500	✓	
-2		.480		600	624	✓	
-3		.467		521	556	✓	
					Avg. 560		
U -4	850	.440	1.280	379	430	✓	
-5		.451	1.279	415	459	✓	
-6		.449	1.279	322	357	✓	
					Avg. 420		
			B - Cycled - 25 ~ Area 1				
C -1	R.T.	.329	1.280	446	675	✓	
-2		.331	1.280	505	759	✓	
					Avg. 720		
C -3	620	.331	1.280	310	466	✓	
-4		.332	1.280	300	450	✓	
					Avg. 460		
C -5	850	.329	1.280	210	318	✓	
-6		.329	1.280	225	340	✓	
					Avg. 330		

Table A-3

UNCONFINED EDGE COMPRESSION PROPERTIES OF CPI MATERIAL WITH 8 AND 12 PERCENT COBALT ADDITIVE

Spec. Ident.	Test Temp. (°C)	Thick (in.)	Width (in.)	Length (in.)	Fail Load (lbs)	Ult. Stress (psi)	Mode of Failure: Catastrophic	Mode of Failure: Center	Mode of Failure: Edge Comp.
				GROUP I - 8% Cobalt					
				A - Uncycled					
U -7	R.T.	.374	.376	.999	480	3400	✓		
-8		.380	.374	.996	514	3620	✓		
-9		.377	.375	.998	528	3740	✓		
						Avg. 3600			
U -1	620	.374	.377	.998	396	2810	✓		
-2		.375	.375	1.000	325	2310		✓	
-3		.375	.375	.986	360	2550	✓		
						Avg. 2600			
U -4	850	.372	.372	.998	213	1540			✓
-5		.380	.376	1.000	246	1720		✓	
-6		.373	.375	.981	249	1780		✓	
						Avg. 1700			
				B - Cycled - 22 ~ Area 2					
C -1	R.T.	.366	.379	.997	468	3370	✓		
-2		.368	.377	1.001	444	3190	✓		
-3		.366	.380	.997	438	3150	✓		
						Avg. 3200			
C -4	620	.367	.381	.997	380	2720		✓	
-5		.367	.380	.997	410	3930		✓	
-6		.367	.380	.997	386	2760		✓	
						Avg. 3100			
C -7	850	.367	.380	.997	274	1960		✓	
-8		.366	.379	.997	406	2920		✓	
-9		.365	.379	.994	372	2700			✓
						Avg. 2500			
				GROUP II - 12% Cobalt					
				A - Uncycled					
U -7	R.T.	.375	.375	1.002	526	3730	✓		
-8		.375	.376	.999	596	4230	✓		
-9		.375	.376	1.001	642	4550		✓	
						Avg. 4200			
U -1	620	.375	.376	1.001	490	3480	✓		
-2		.372	.375	.999	359	2560	✓		
-3		.377	.375	1.001	523	3780		✓	
						Avg. 3300			
U -4	850	.375	.373	1.001	400	2860		✓	
-5		.375	.373	1.001	320	2290	✓		
-6		.375	.374	1.001	337	2410		✓	
						Avg. 2500			
				B - Cycled -25 ~ Area 1					
C -1	R.T.	.331	.366	.996	425	3510			✓
-2		.330	.367	.999	390	3220			✓
-3		.330	.366	.998	410	3390		✓	
						Avg. 3400			
C -4	620	.332	.366	.997	200	1640	✓		
-5		.330	.366	.997	172	1420	✓		
-6		.332	.366	.997	174	1430	✓		
						Avg. 1500			
C -7	850	.332	.366	.997	253	2070		✓	
-8		.332	.366	.999	192	1570		✓	
-9		.331	.366	.996	202	1670		✓	
						Avg. 1800			

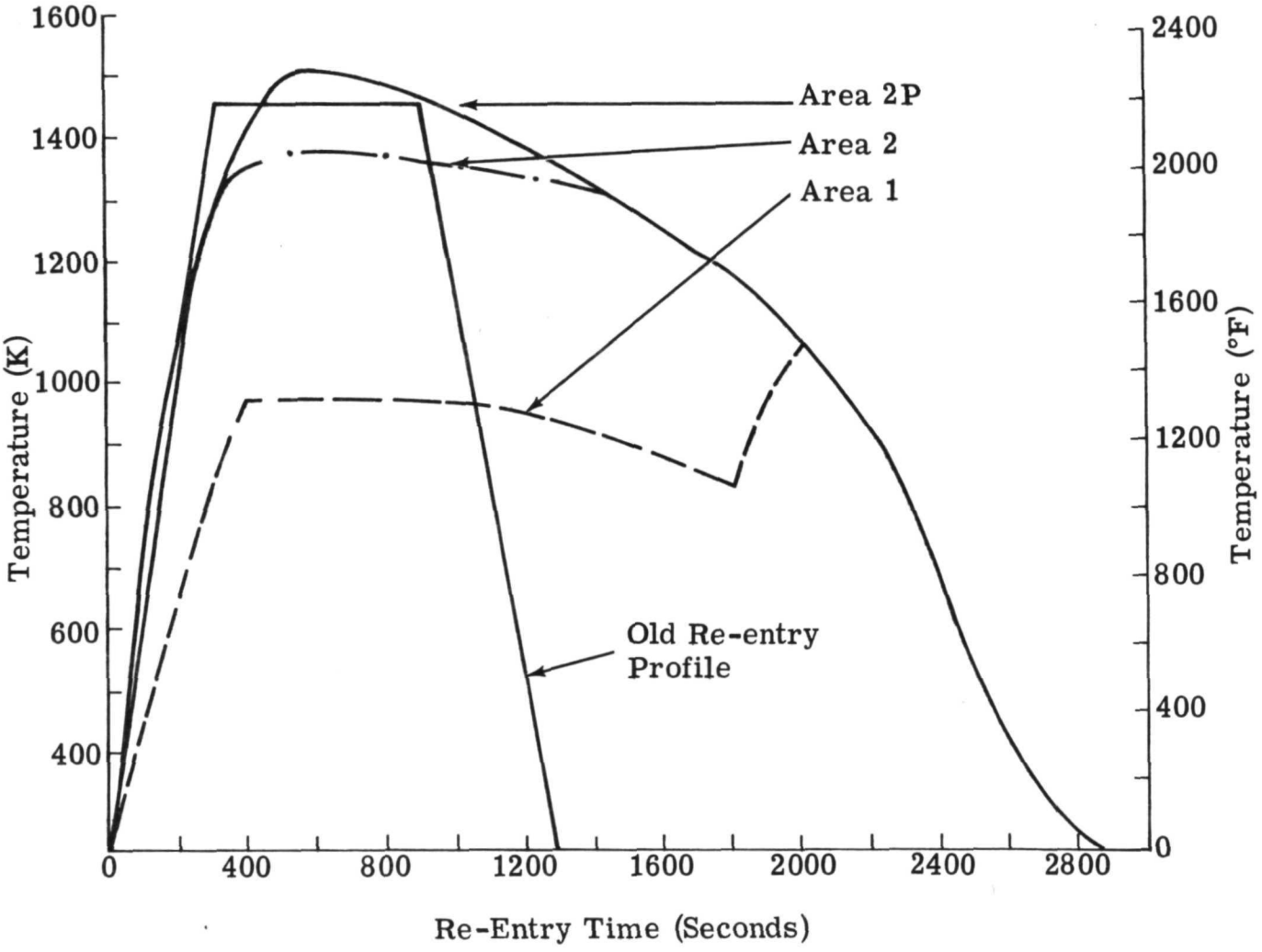

Fig. 1 Modified Re-Entry Thermal Profiles

Legend:

Area	Samples
A	Diametral Compression and Emittance
B	Thermal Conductivity
C	Free Standing Compression
D	Wat. Abs., X-ray, Etc.
E	Flexure
F	Thermal Expansion

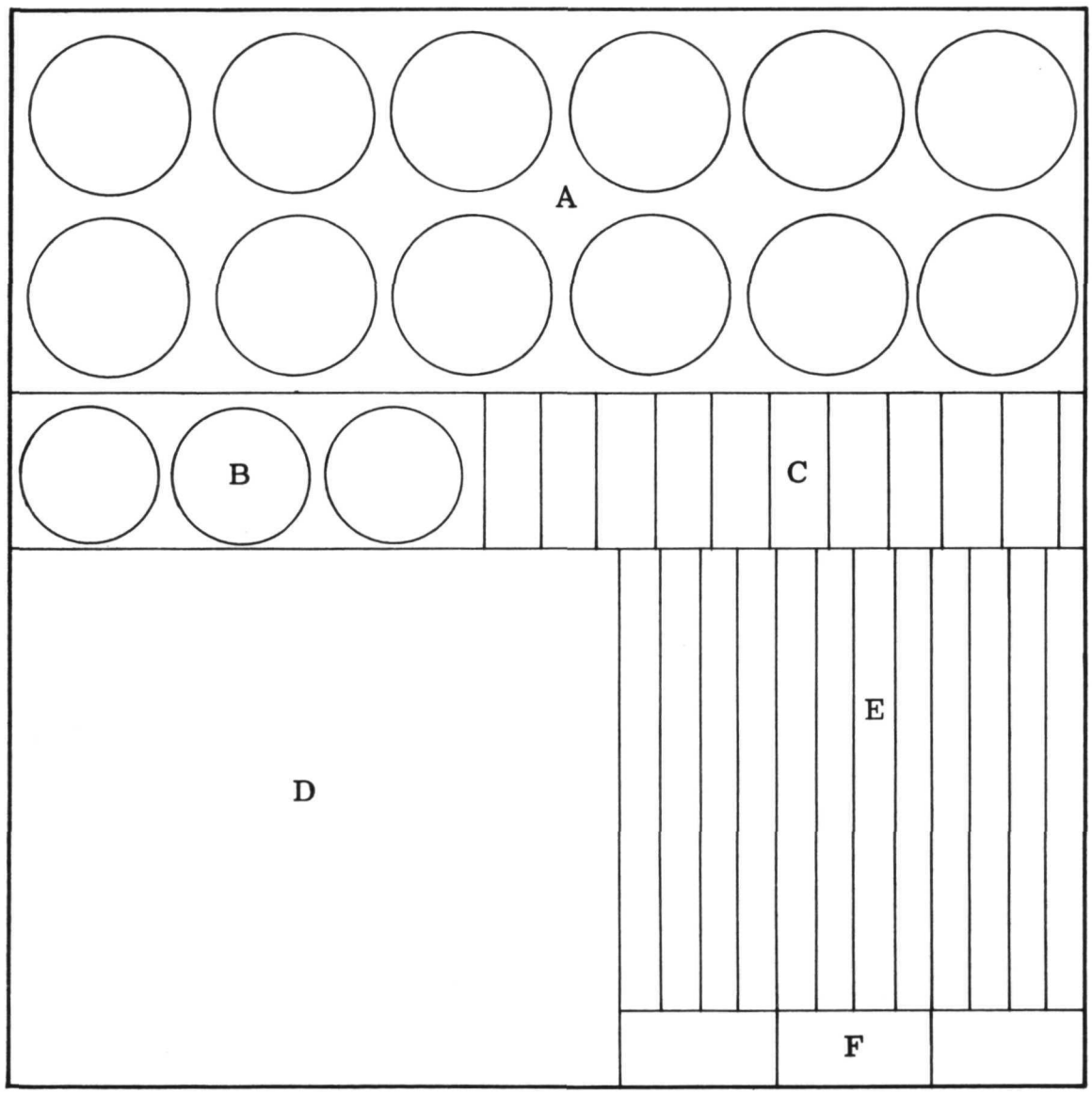

Fig. 2 Samples Cut from CPI Tiles

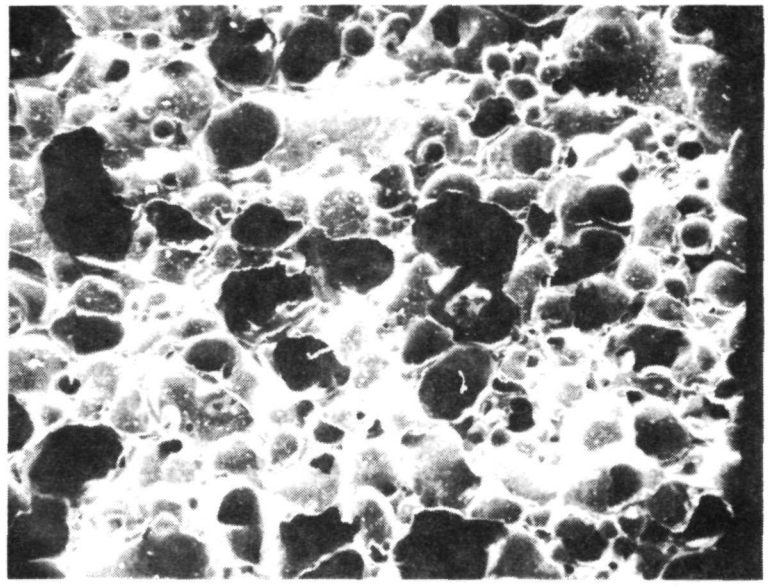

CPI 8 Cycled 25 Times Area 2 (50X)

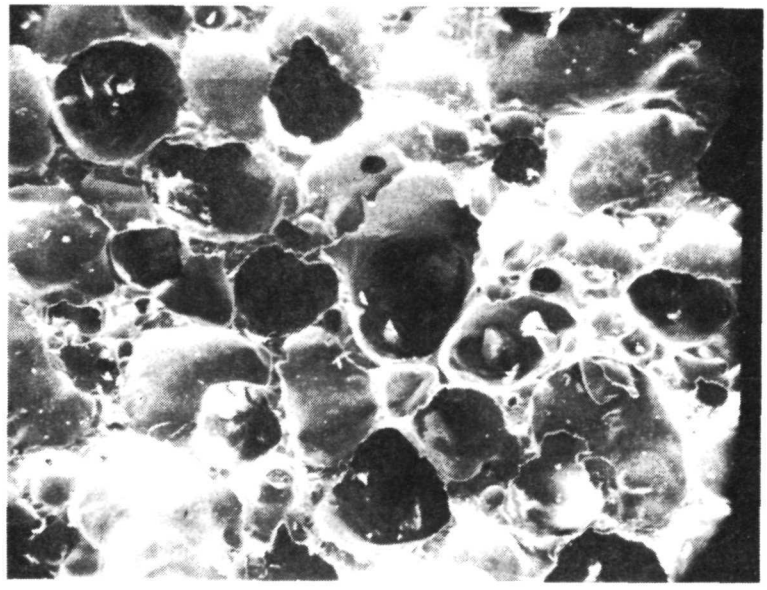

CPI 12 Cycled 25 Times Area 1 (50X)

Fig. 3 Scanning Electron Micrographs of CPI-12 and CPI-8 after Thermal Cycling

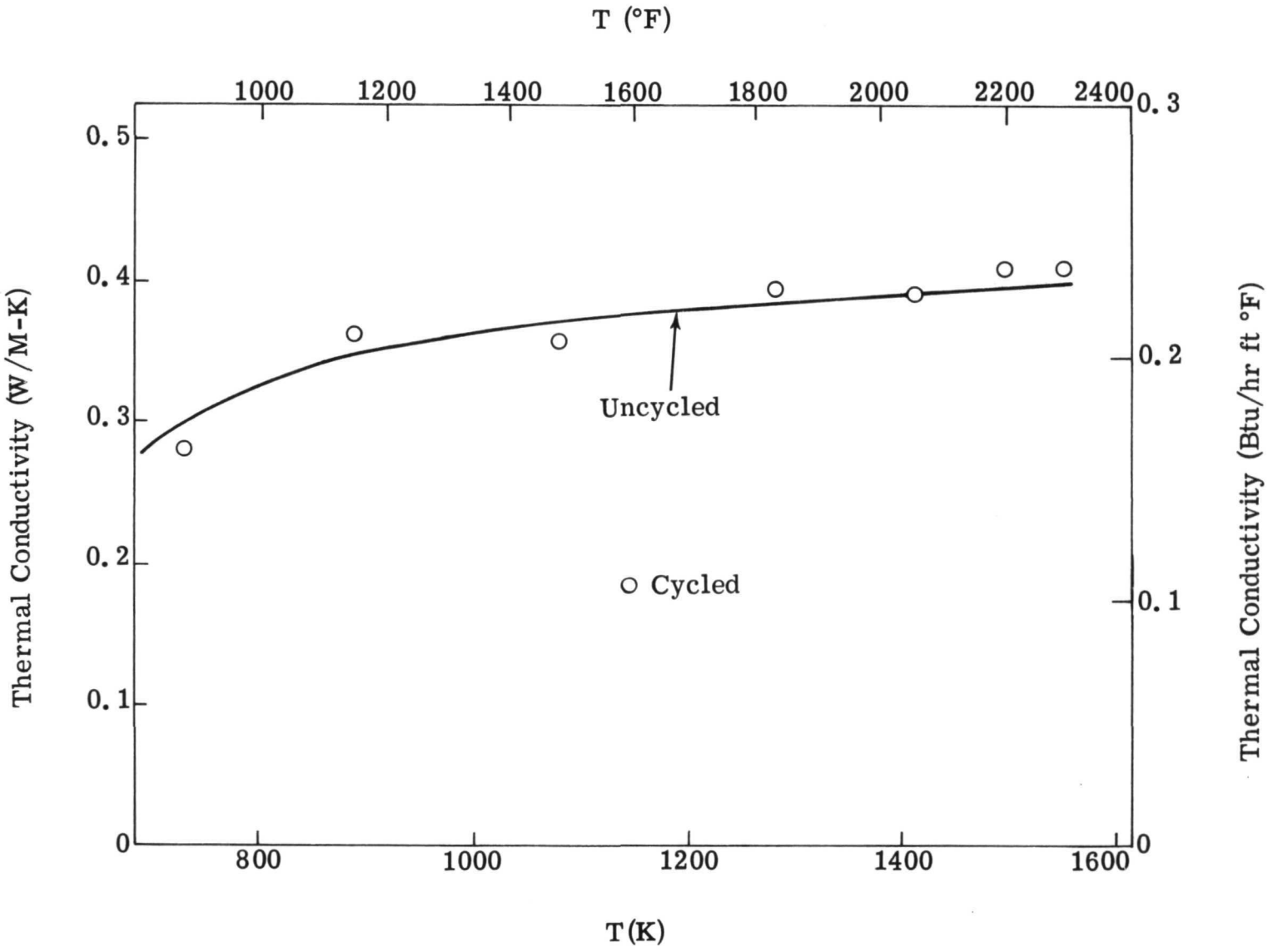

Thermal Conductivity versus Temperature for CPI-12

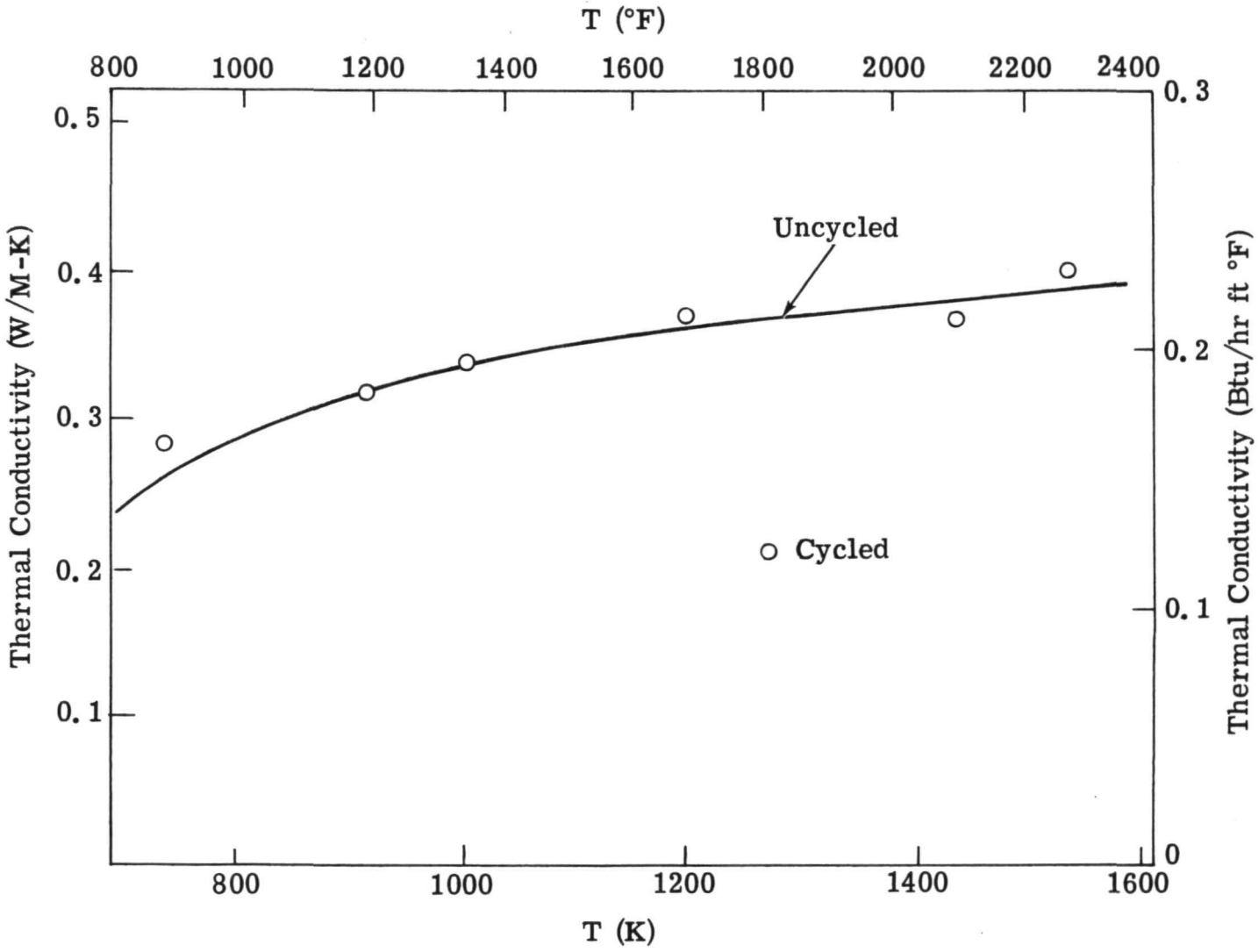

Fig. 5 Thermal Conductivity versus Temperature for CPI-8

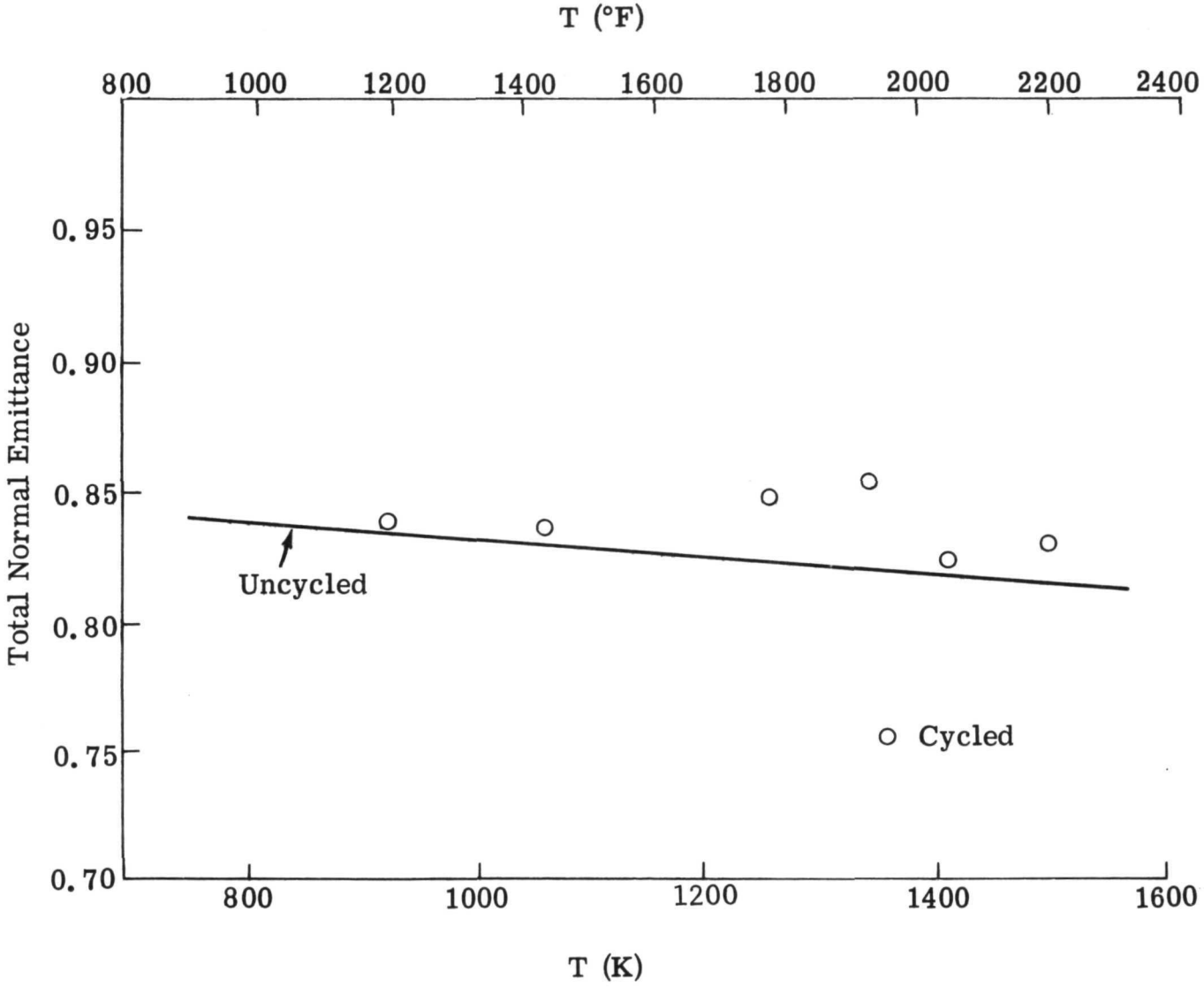

Fig. 6 Total Normal Emittance versus Temperature for CPI-12

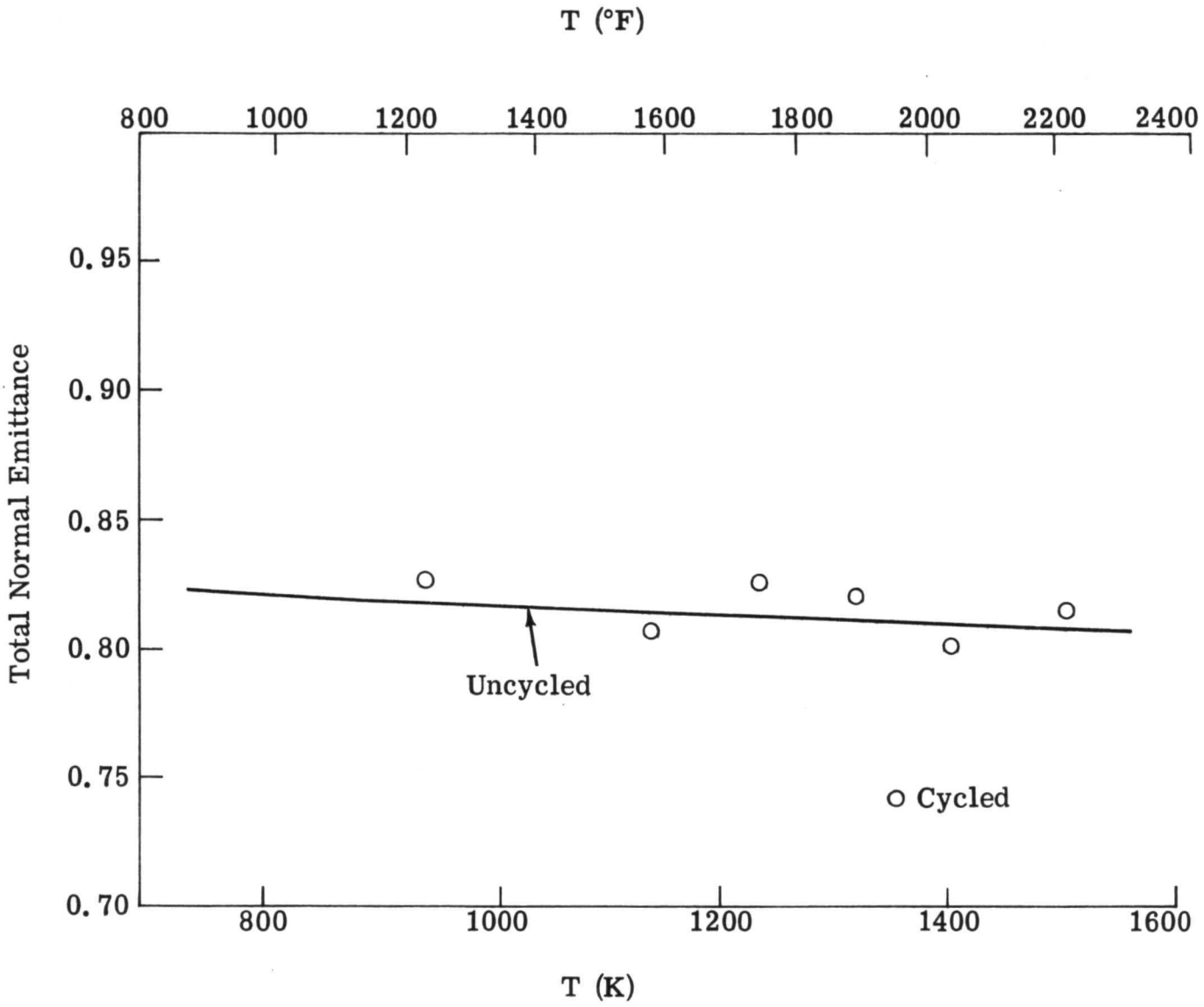

Fig. 7 Total Normal Emittance versus Temperature for CPI-8

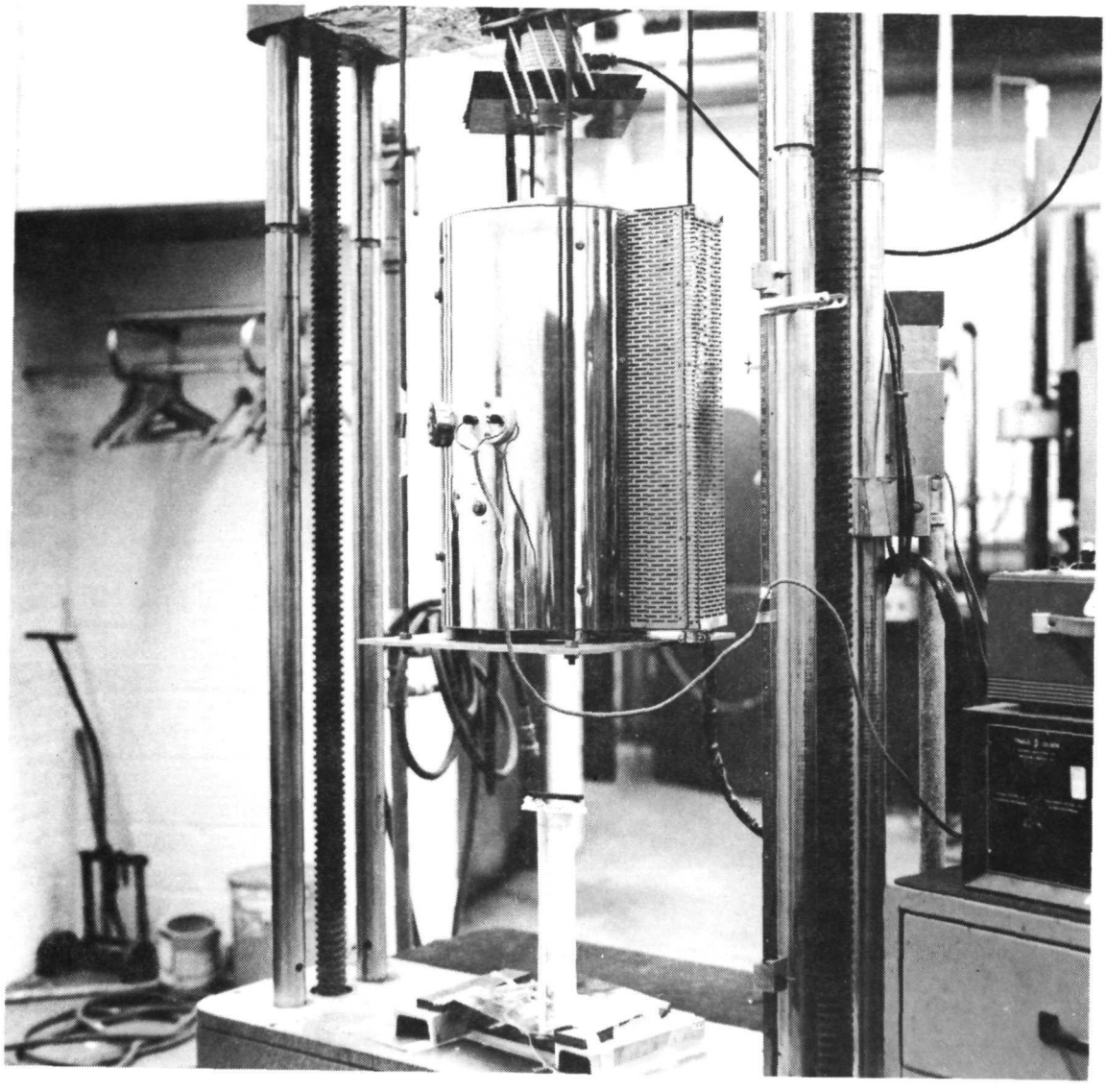

Fig. 8 Elevated Temperature Fixturing for Flexure Test

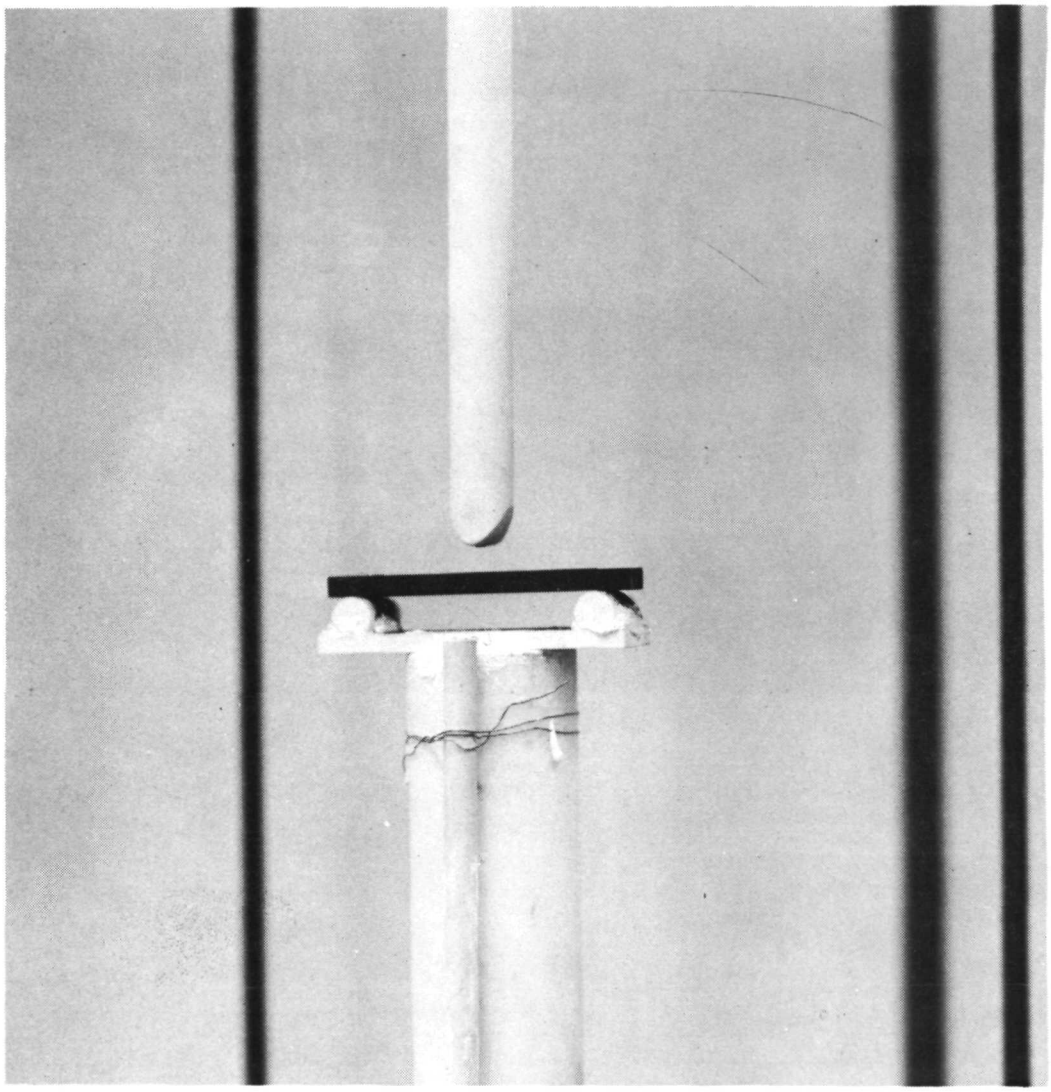

Fig. 9 Close-up of Elevated Temperature Fixturing for Flexure Test

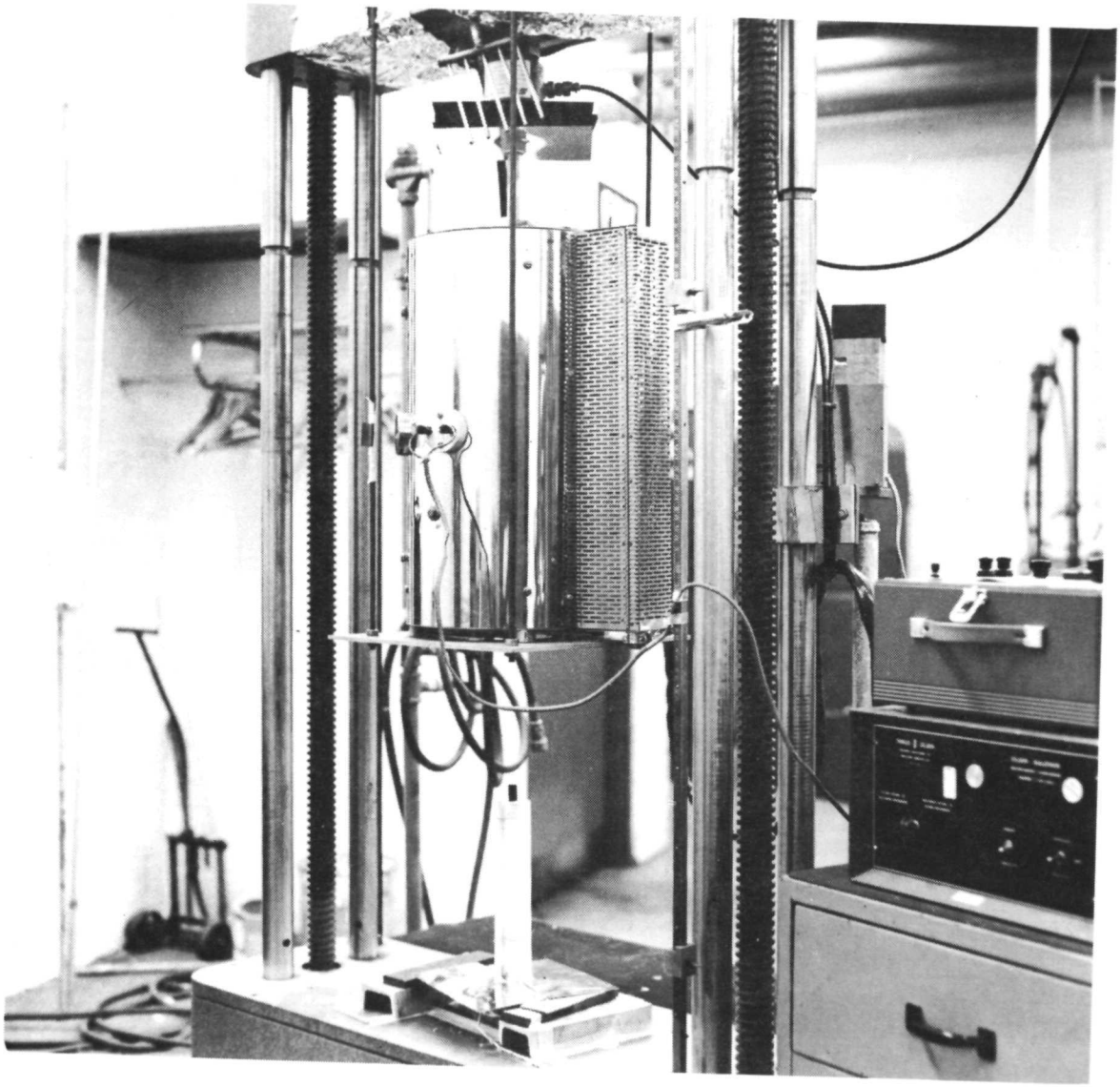

Fig. 10 Elevated Temperature Fixturing for Edge Compression Test

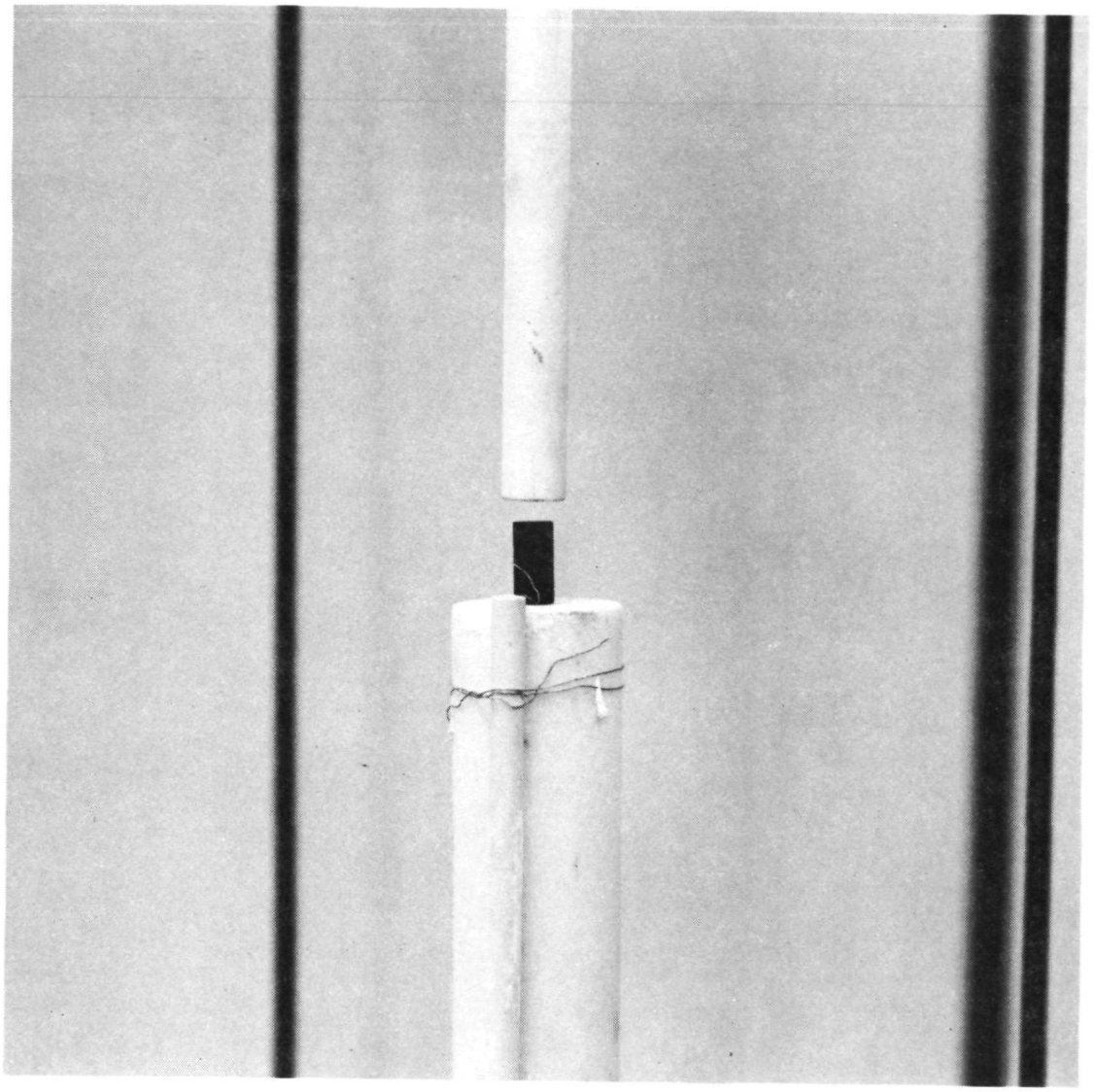

Fig. 11 Close-up Elevated Temperature Fixturing for Edge Compression Test

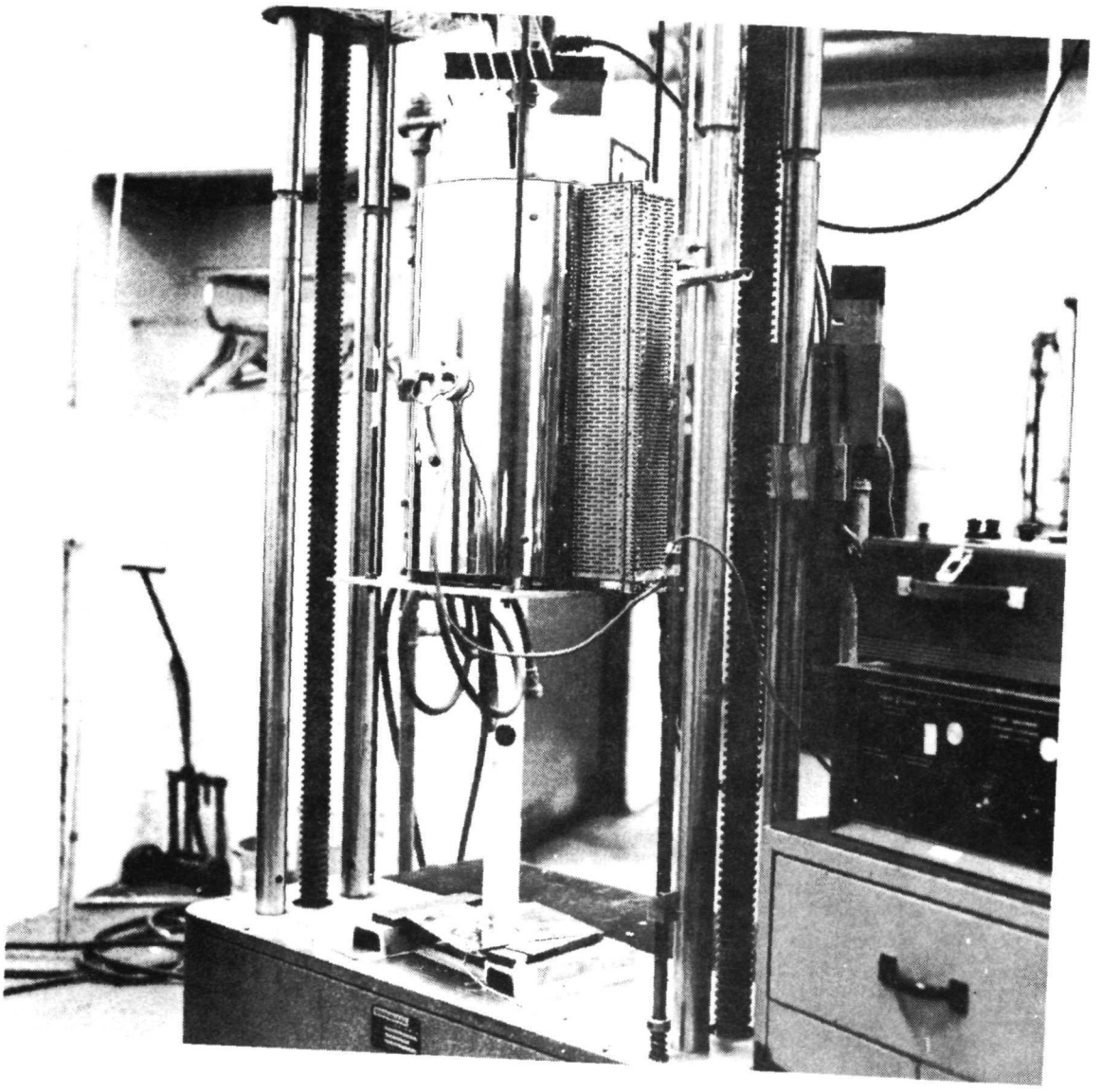

Fig. 12 Elevated Temperature Fixturing for Diametral Compression (Tension) Test

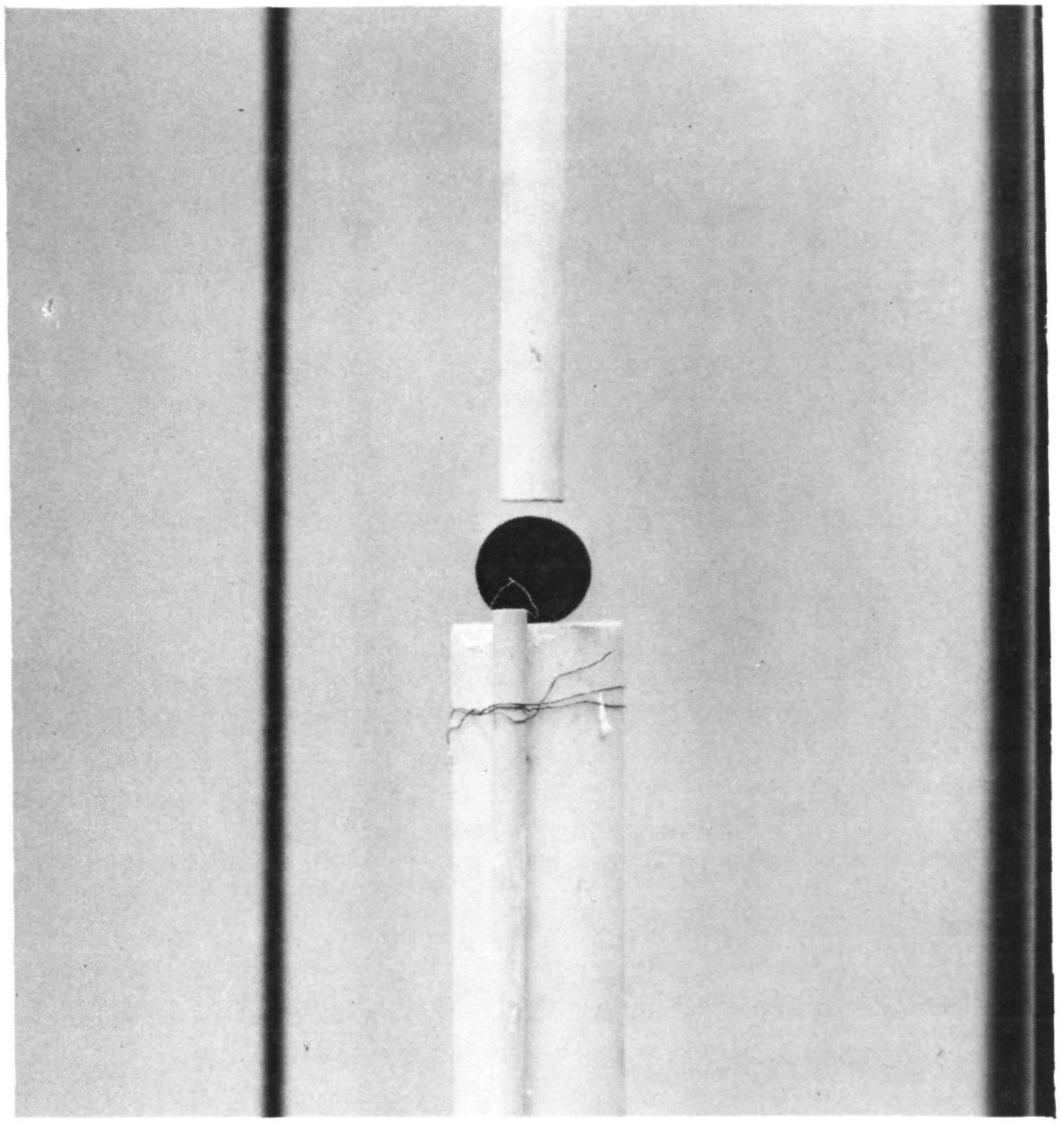

Fig. 13 Close-up of Elevated Temperature Fixturing for Diametral Compression Test

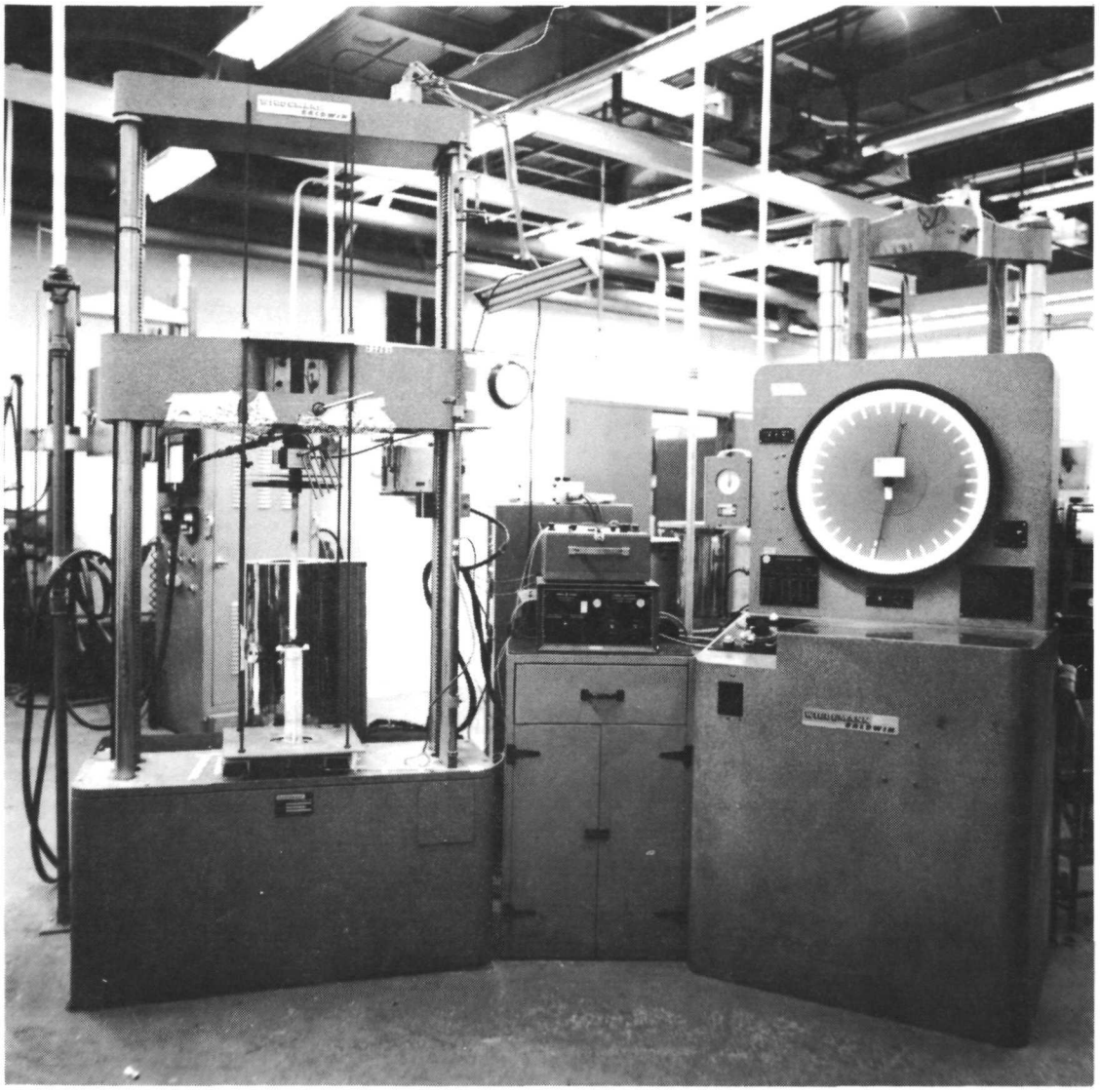

Fig. 14 Over-all View of Universal Testing Machine, Furnace and Test Fixtures

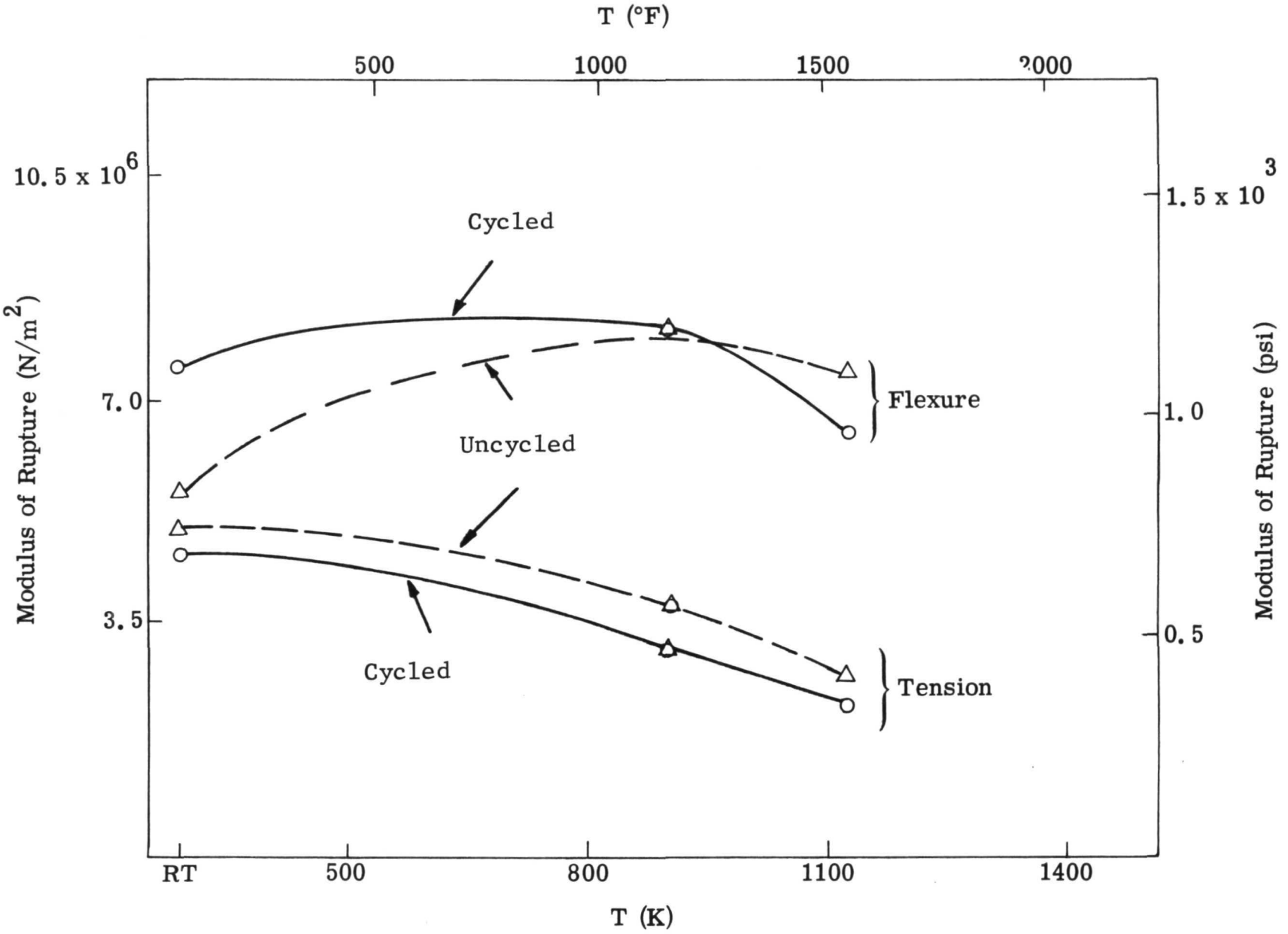

Fig. 15 Flexure and Tensile Strengths versus Temperature for CPI-12

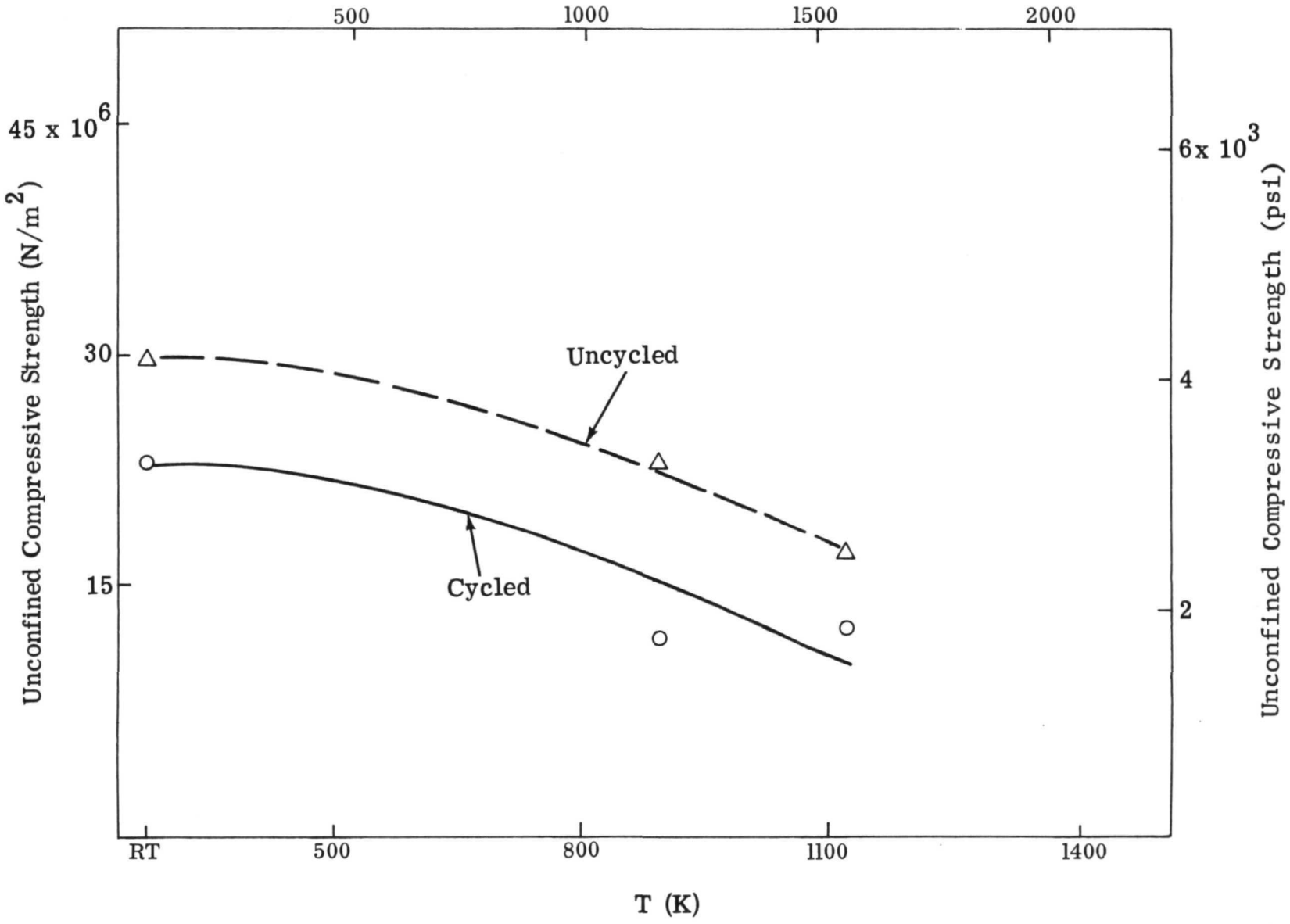

Fig. 16 Compressive Strength versus Temperature for CPI-12

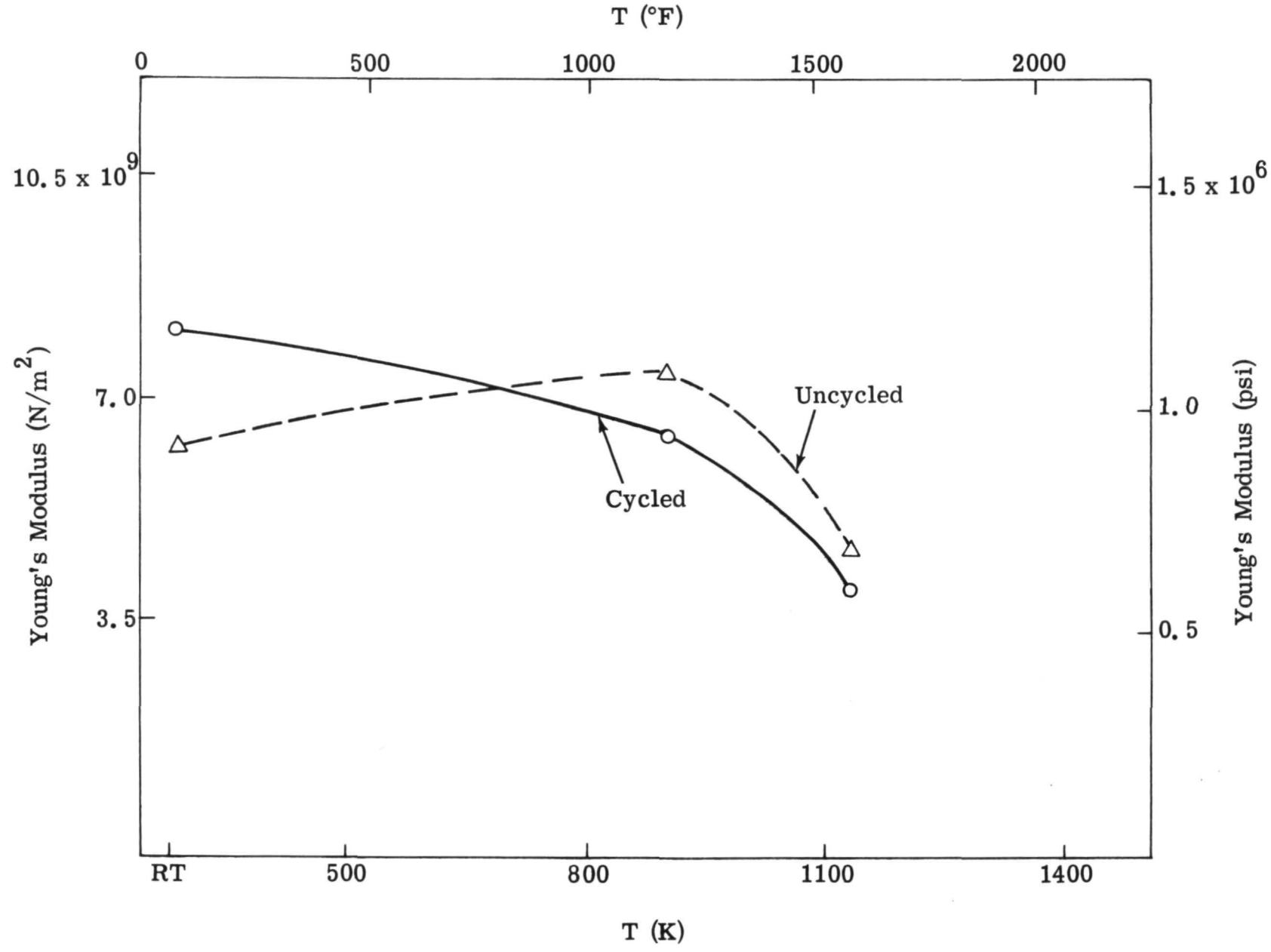

Fig. 17 Young's Modulus versus Temperature for CPI-12

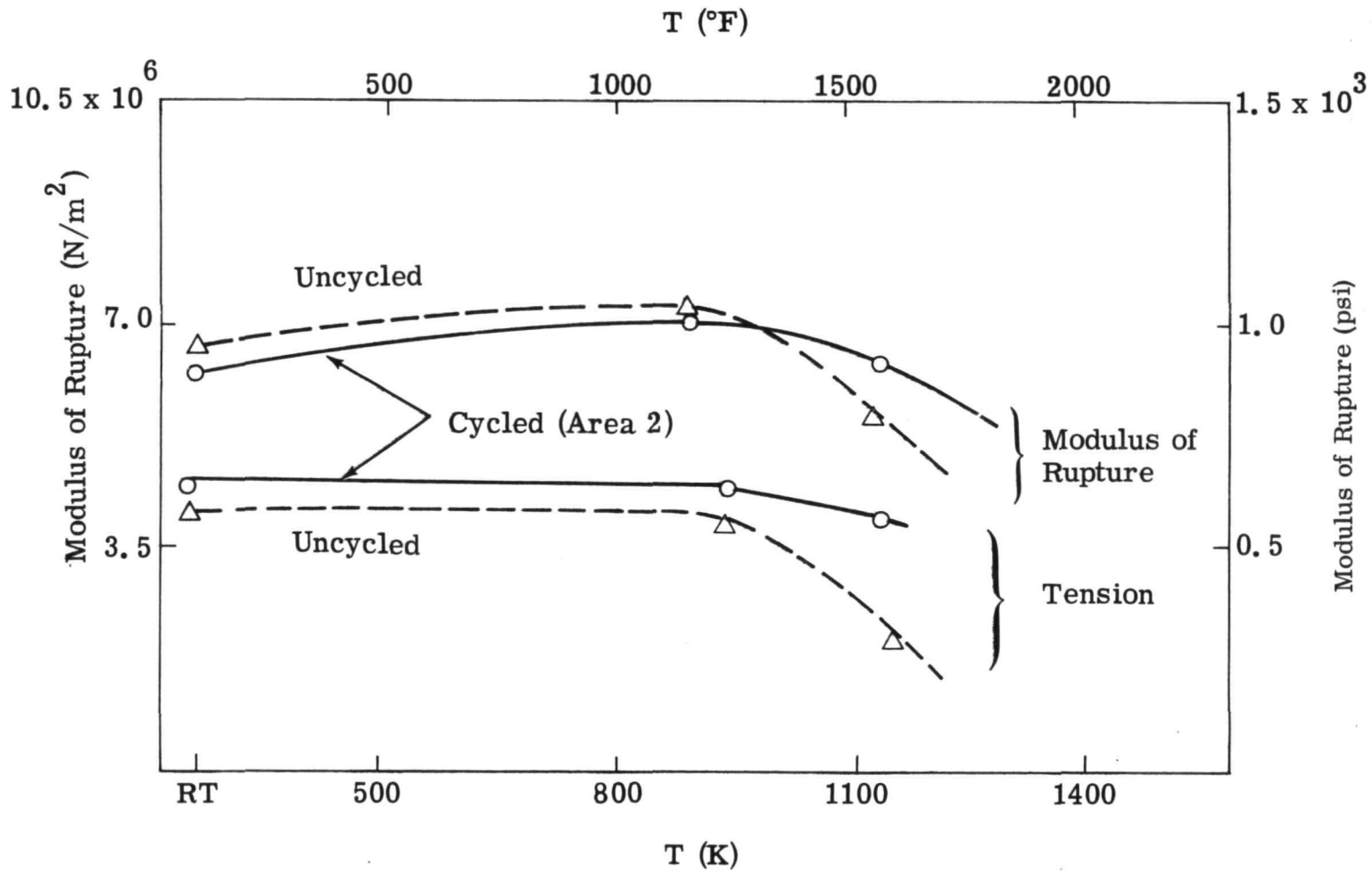

Fig. 18 Flexure and Tensile Strengths versus Temperature for CPI-8

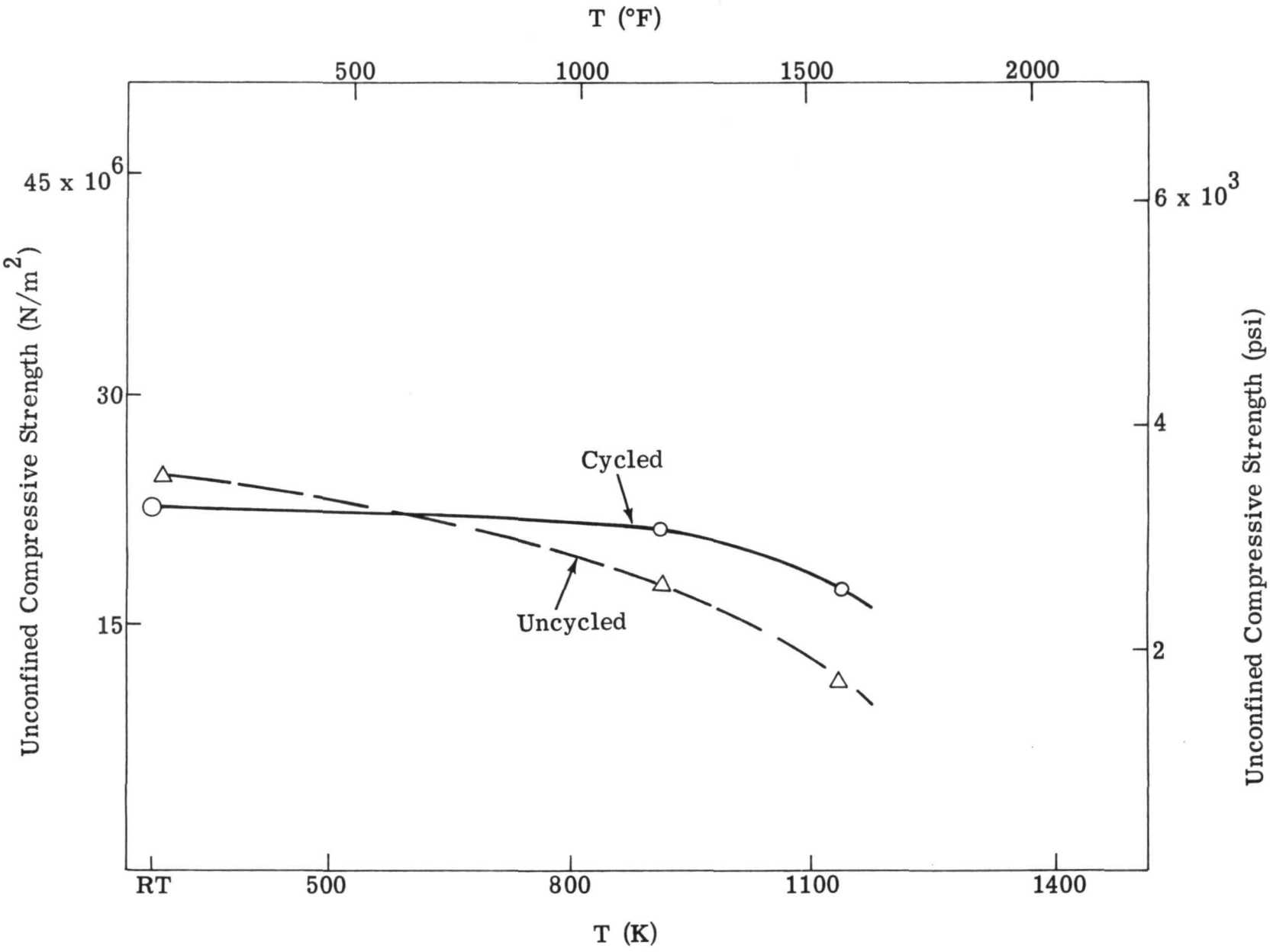

Fig. 19 Compressive Strength versus Temperature for CPI-8

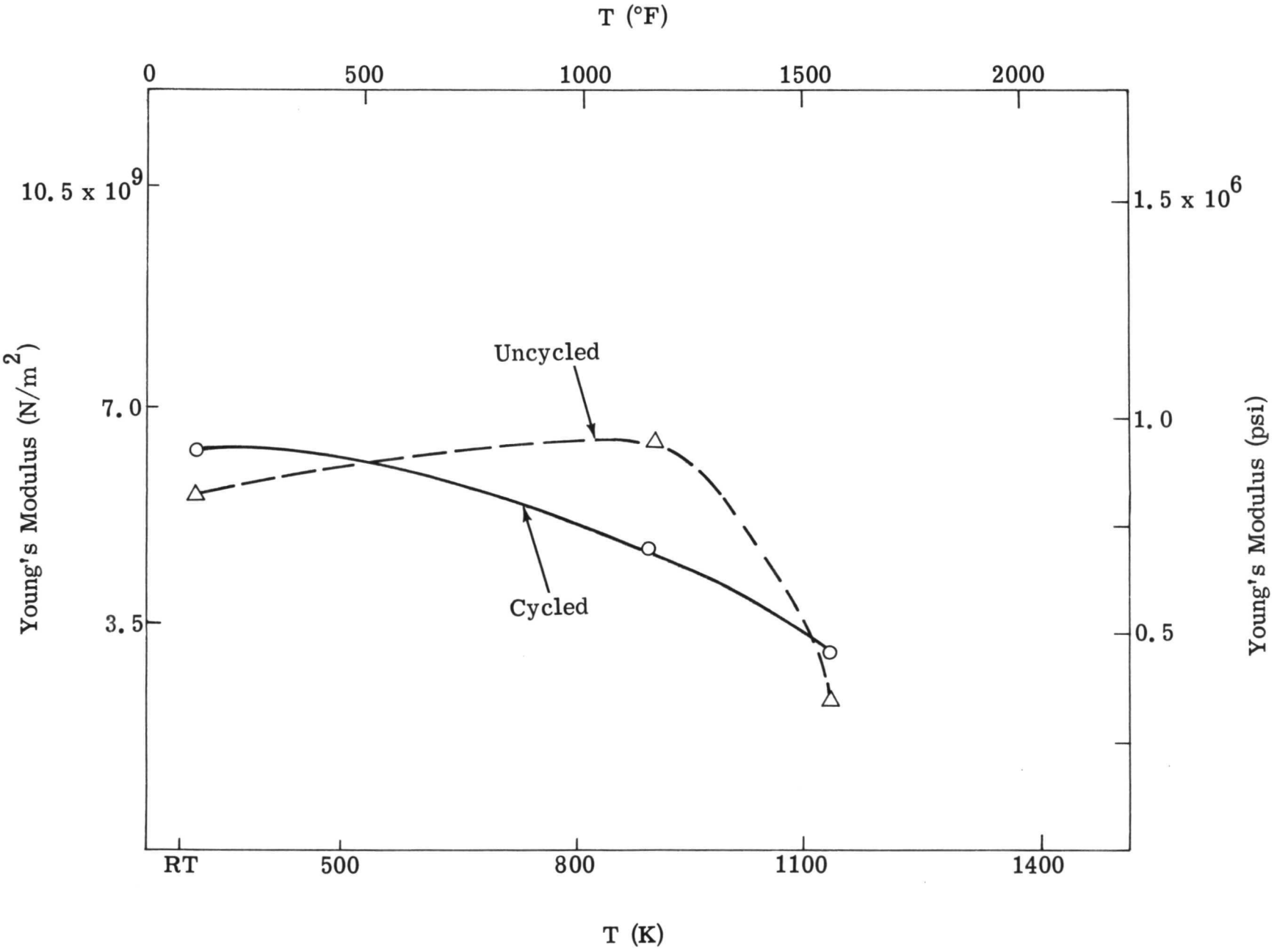

Fig. 20 Youngs Modulus versus Temperature for CPI-8

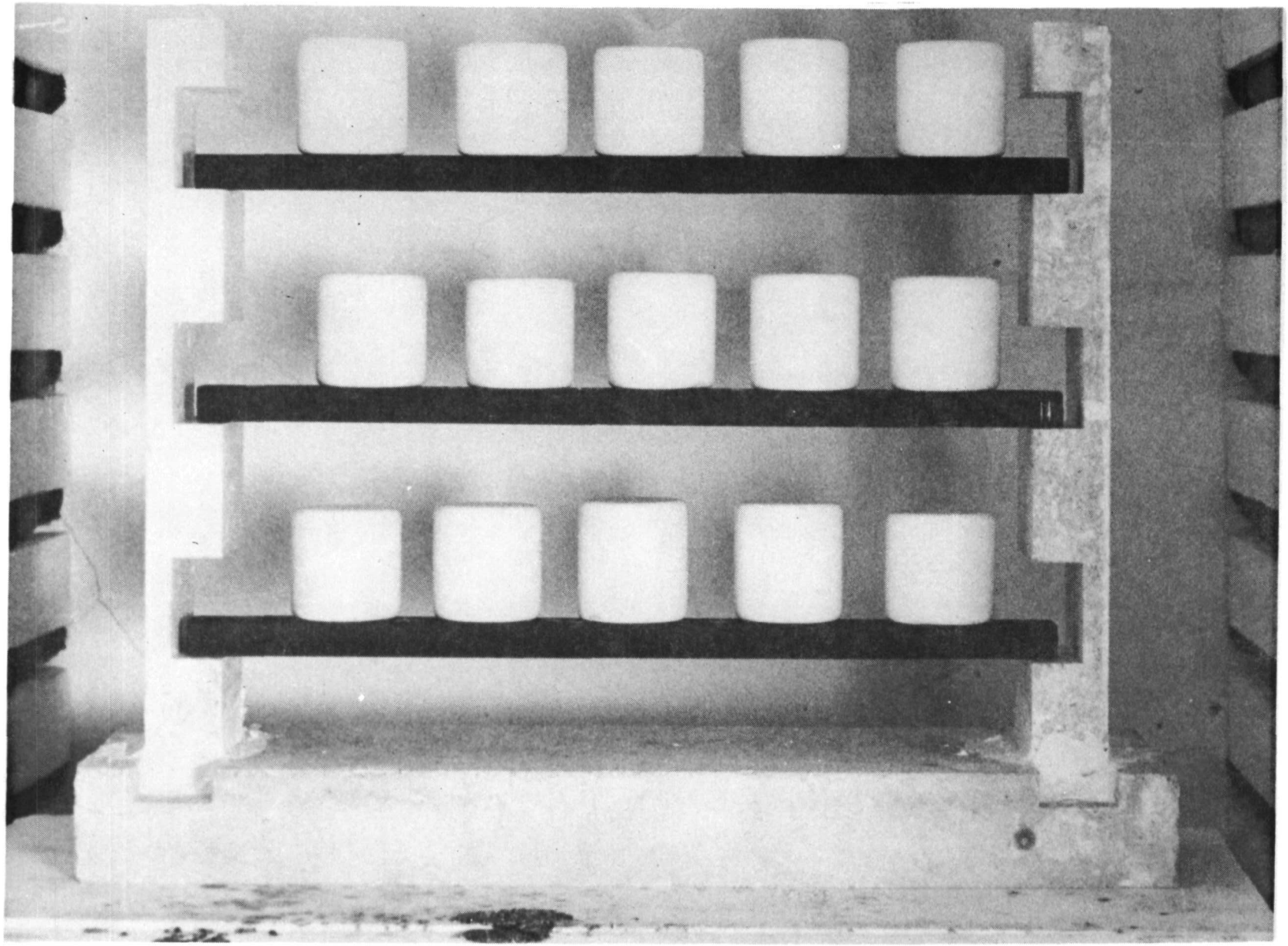

Fig. 21 Setup Showing Loaded Beams for Creep Study before Testing

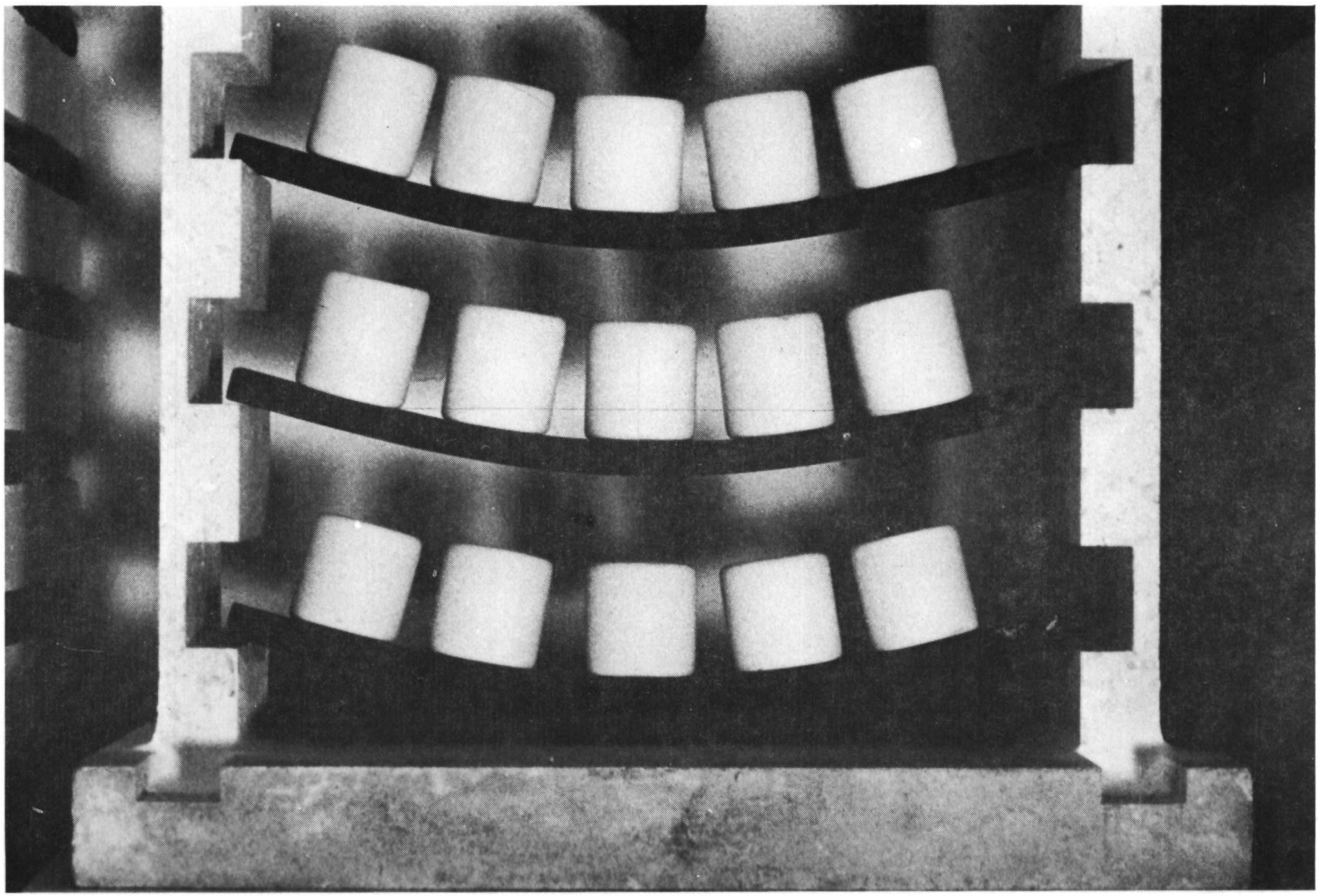

Fig. 22 CPI-8 Beams After 18 Hours at 1253 K

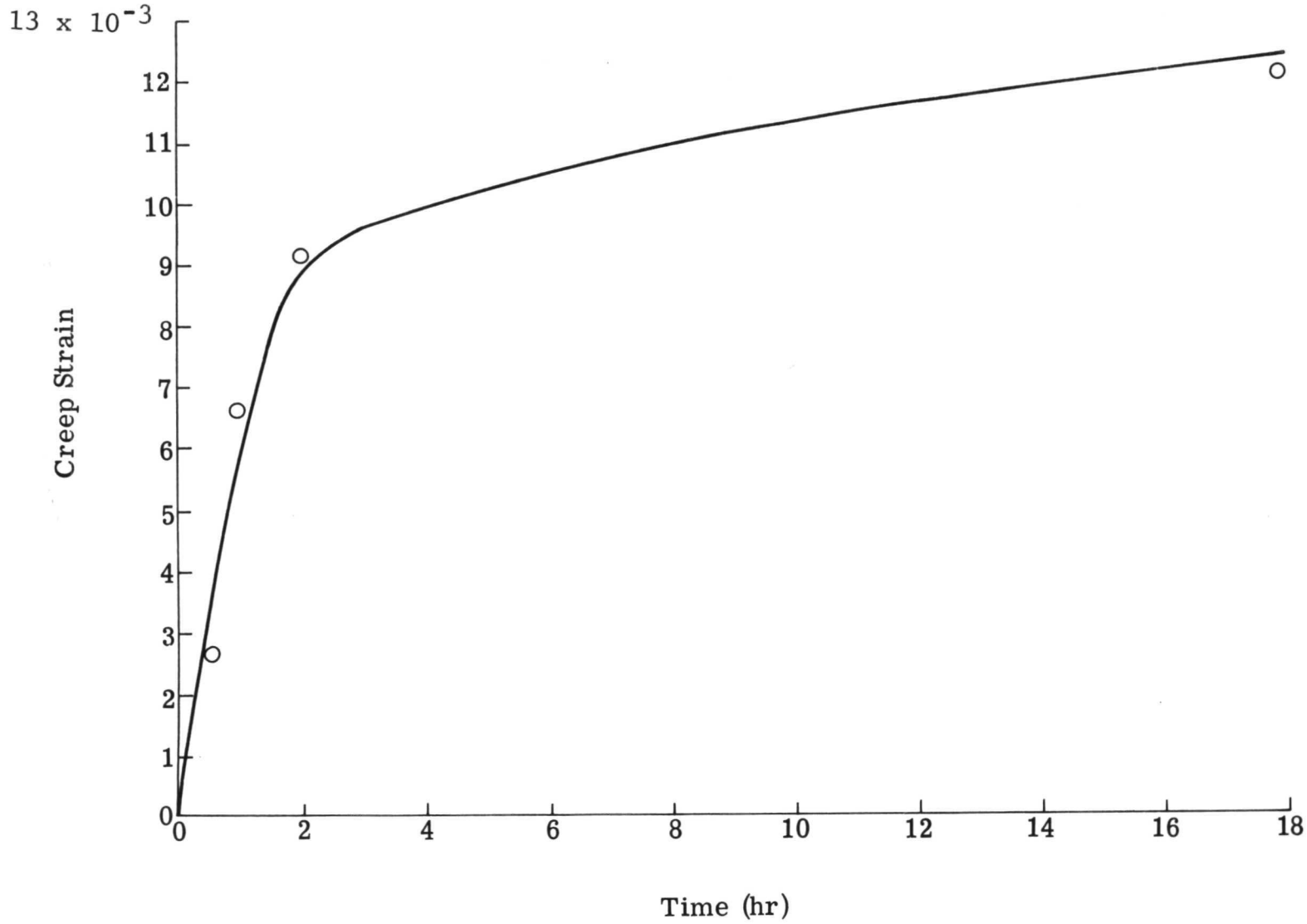

Fig. 23 Flexural Creep Strain versus Time for CPI-8 at 1253 K